CYANIDE FLUORESCENT SENSORS FROM INDOLIUM-FLUOROPHORE CONJUGATES

Miss Siraporn Soonthonhut

จุฬาลงกรณ์มหาวิทยาลัย
CHULALONGKORN UNIVERSITY

A Dissertation Submitted in Partial Fulfillment of the Requirements
for the Degree of Doctor of Philosophy in Chemistry
Department of Chemistry
FACULTY OF SCIENCE
Chulalongkorn University
Academic Year 2022
Copyright of Chulalongkorn University

ไซยาไนด์ฟลูออเรสเซนต์เซ็นเซอร์จากอินโดเลียม-ฟลูออโรฟอร์คอนจูเกต

น.ส.ศิราภรณ์ สุนทรหุต

จุฬาลงกรณ์มหาวิทยาลัย
CHULALONGKORN UNIVERSITY

วิทยานิพนธ์นี้เป็นส่วนหนึ่งของการศึกษาตามหลักสูตรปริญญาวิทยาศาสตรดุษฎีบัณฑิต
สาขาวิชาเคมี ภาควิชาเคมี
คณะวิทยาศาสตร์ จุฬาลงกรณ์มหาวิทยาลัย
ปีการศึกษา 2565
ลิขสิทธิ์ของจุฬาลงกรณ์มหาวิทยาลัย

Thesis Title	CYANIDE FLUORESCENT SENSORS FROM INDOLIUM-FLUOROPHORE CONJUGATES
By	Miss Siraporn Soonthonhut
Field of Study	Chemistry
Thesis Advisor	Professor PAITOON RASHATASAKHON, Ph.D.
Thesis Co Advisor	Professor MONGKOL SUKWATTANASINITT, Ph.D.

Accepted by the FACULTY OF SCIENCE, Chulalongkorn University in Partial Fulfillment of the Requirement for the Doctor of Philosophy

..... Dean of the FACULTY OF SCIENCE
(Professor POLKIT SANGVANICH, Ph.D.)

DISSERTATION COMMITTEE

..... Chairman
(Professor PATCHANITA THAMYONGKIT, Ph.D.)

..... Thesis Advisor
(Professor PAITOON RASHATASAKHON, Ph.D.)

..... Thesis Co-Advisor
(Professor MONGKOL SUKWATTANASINITT, Ph.D.)

..... Examiner
(Professor THAWATCHAI TUNTULANI, Ph.D.)

..... Examiner
(Professor BUNCHA PULPOKA, Ph.D.)

..... External Examiner
(Associate Professor Nakorn Niamnont, Ph.D.)

จุฬาลงกรณ์มหาวิทยาลัย
Chulalongkorn University

ศิราภรณ์ สุนทรหุต : ไซยาไนด์ฟลูออเรสเซนต์เซ็นเซอร์จากอินโดเลียม-ฟลูออโรฟอร์คอนจูเกต. (CYANIDE FLUORESCENT SENSORS FROM INDOLIUM-FLUOROPHORE CONJUGATES) อ.ที่ปรึกษาหลัก : ศ. ดร.ไพฑูรย์ รัชตะสาคร, อ.ที่ปรึกษาร่วม : ศ. ดร.มงคล สุขวัฒนาสินิทธิ์

งานวิจัยนี้มีการออกแบบและพัฒนาอนุพันธ์ของอินโดเลียมที่เชื่อมต่อกับฟลูออโรฟอร์ 3 ชนิด ได้แก่ จูโลลิดีน, ไตรเฟนิลลามีน, และไพรีน ได้เป็นสารอนุพันธ์ INJ, INT และ INP ตามลำดับ กระบวนการสังเคราะห์ทำผ่านปฏิกิริยายาควบแน่นได้ร้อยละผลผลิตมากกว่า 80% อนุพันธ์ทั้ง 3 ชนิดได้รับการยืนยันโครงสร้างและทดสอบคุณสมบัติทางแสงพบว่ามีค่าประสิทธิภาพเชิงควอนตัมทางฟลูออเรสเซนต์ที่ต่ำ อนุพันธ์ทั้งหมดแสดงให้เห็นถึงความจำเพาะเจาะจงในการเลือกจับกับไซยาไนด์ทั้งในรูปแบบคัลเลอริเมตริกและฟลูออเรสเซนต์ซึ่งเป็นผลอันเนื่องมาจากกระบวนการชาร์จทรานเฟอร์ภายในโมเลกุล (ICT) ถูกขัดขวาง ความว่องไวในการตรวจจับไซยาไนด์ของอนุพันธ์ทั้งสามถูกคำนวนออกมาทั้งในรูปแบบคัลเลอริเมตริกและฟลูออเรสเซนต์ให้ผลว่า อนุพันธ์ INJ และ INT มีความว่องไวในการตรวจวัดสูงซึ่งสามารถทำงานได้ในการตรวจวัดความเข้มข้นของไซยาไนด์ที่ระดับต่ำกว่า EPA กำหนด กลไกการเกิดสารประกอบระหว่างอนุพันธ์กับไซยาไนด์สามารถตรวจสอบได้ด้วย ^{1}H-NMR, การทดลองหาปริมาณสัมพันธ์ (Job's plot), และแมสสเปกโตรเมตรี จากผล ^{1}H-NMR พบว่าไซยาไนด์เข้าทำปฏิกิริยาการเติมด้วยนิวคลีโอไฟล์ที่ตำแหน่ง 1,2 และผลการทดลองหาปริมาณสัมพันธ์ยืนยันอัตราส่วนการเข้าทำปฏิกิริยาที่ 1:1 เนื่องด้วยระดับความเข้มข้นต่ำสุดที่สามารถตรวจวัดได้ (LOD) ของอนุพันธ์ INT นั้นมีค่าอยู่ที่ 24 นาโนโมลาร์ในสารละลายน้ำ จึงได้นำไปประยุกต์ใช้ตรวจสอบปริมาณไซยาไนด์ในตัวอย่างน้ำซึ่งให้พบการตรวจสอบที่แม่นยำและเที่ยงตรงโดยมีร้อยละการกลับคืนอยู่ที่ 98-106% นอกจากนี้ยังมีการทดลองใช้อนุพันธ์ในการทดสอบเบื้องต้นเพื่อหาปริมาณไซยาไนด์บนตัวตรวจวัดแบบกระดาษได้สำเร็จ

สาขาวิชา เคมี	ลายมือชื่อนิสิต .....
ปีการศึกษา 2565	ลายมือชื่อ อ.ที่ปรึกษาหลัก .....
	ลายมือชื่อ อ.ที่ปรึกษาร่วม .....

6072830023 : MAJOR CHEMISTRY

KEYWORD: Cyanide, fluorescence sensor, indolium ion, julolidine, triphenylamine, pyrene

Siraporn Soonthonhut : CYANIDE FLUORESCENT SENSORS FROM INDOLIUM-FLUOROPHORE CONJUGATES. Advisor: Prof. PAITOON RASHATASAKHON, Ph.D. Co-advisor: Prof. MONGKOL SUKWATTANASINITT, Ph.D.

Indolium conjugated with three fluorophores including julolidine, triphenylamine, and pyrene (INJ, INT, INP) were successfully synthesized via condensation reaction with an excellent yield over 80%. All of derivatives were fully characterized and investigated the photophysical properties revealing that synthesized indolium-fluorophore conjugates has a negligible quantum yield. All synthesized compounds expressed the great selectivity toward cyanide ion indicating by colorimetric and fluorescence signal change due to internal charge transfer process (ICT) was interrupted. The sensitivity on cyanide detection was carried on both colorimetric and fluorescence mode resulting the excellent sensitivity on INT and INJ which can be operated for analysis of cyanide concentration that lower than EPA guidance. ^{1}H-NMR, Job's plot and mass spectrometry were used to confirm the sensing mechanism between indolium-fluorophore conjugates and cyanide. ^{1}H-NMR indicated the 1,2-nucleophilic addition of cyanide with 1:1 ratio that provided by Job's plot pattern. With the lowest LOD at 24 nM on fluorescence mode in aqueous system, INT was applied for real water samples analysis illustrating the high accuracy and precision with 98-106% recovery. Moreover, the preliminary result of convenient paper-based sensor for cyanide analysis was carried out successfully.

จุฬาลงกรณ์มหาวิทยาลัย
Chulalongkorn University

Field of Study: Chemistry
Academic Year: 2022

Student's Signature .....
Advisor's Signature .....
Co-advisor's Signature .....

ACKNOWLEDGEMENTS

At first and foremost, I would like to express my deep gratitude to my thesis advisor, Professor Dr. Paitoon Rashatasakhon, and my thesis Co-Advisor Professor Dr. Mongkol Sukwattanasinitt, for the research opportunities, kindness, valuable advices, and the excellent guidance and encouragement thorough this research. This work would not be completed without their support.

I would like to extend my sincere thanks to the Ph.D thesis defense committee, Professor Dr. Patchanita Thamyongkit, Professor Dr. Thawatchai Tuntulani, Professor Dr. Buncha Pulpoka and Associate Professor Dr. Nakorn Niamnont for their beneficial suggestion, and recommendations.

Furthermore, my appreciation is giving to Dr. Kannikar Vongnam, Dr. Tianchai Chooppawa and Dr. Komthep Silpharu, for their helpful, suggestions and guidance. I also would like to thanks Dr. Nichapa Chanawungmuang, Dr. Voravin Asavasuthiphan, Dr. Warakorn Akarasareenon, Mr. Thanadech Nilket, Ms. Quynh Pham Nguyen Nhu, and Mr. Yuttana Senpradit who are the best colleagues that I had the most pleasure to working with. Moreover, I gratefully thank to everyone in MAPS group for the friendship, and their helps in everything.

I would like to acknowledge Science Achievement Scholarship of Thailand (SAST) for the financial support thorough the whole study program.

Lastly, I would be remiss in not mentioning my beloved family who always stand by my side on both my pleasant and hard time

Siraporn Soonthonhut

จุฬาลงกรณ์มหาวิทยาลัย
Chulalongkorn University

TABLE OF CONTENTS

Page

.....iii

ABSTRACT (THAI).....iii

.....iv

ABSTRACT (ENGLISH).....iv

ACKNOWLEDGEMENTS.....v

TABLE OF CONTENTS.....vi

LIST OF TABLES.....ix

LIST OF FIGURES.....x

CHAPTER I INTRODUCTION.....1

1.1 Fluorescence.....1

1.2 Fluorescence sensor.....2

1.3 Sensing Mechanism.....3

1.4 Literature reviews.....4

1.4.1 Fluorescence sensor based on Indolium unit for cyanide detection.....4

1.4.2 Signaling unit for fluorescence sensor.....10

1.5 Objectives of this research.....17

CHAPTER II EXPERIMENTAL.....19

2.1 Reagents and materials.....19

2.2 Methods.....19

2.2.1 UV-Visible spectroscopy.....19

2.2.2 Fluorescence spectroscopy.....20

จุฬาลงกรณ์มหาวิทยาลัย
Chulalongkorn University

2.2.3 ^{1}H and ^{13}C spectroscopy 20

2.2.4 Mass spectroscopy 20

2.3 Synthesis and characterization 20

2.3.1 1,2,3,3-Tetramethyl-3H-indolium iodide 20

2.3.2 (E)-2-(2-(1,2,3,5,6,7-hexahydropyrido[3,2,1-ij]quinolin-9-yl)vinyl)-1,3,3-trimethyl-3H-indol-1-ium (INJ) 21

2.3.3 4-(diphenylamino) benzaldehyde 22

2.3.4 (E)-2-(4-(diphenylamino)styryl)-1,3,3-trimethyl-3H-indol-1-ium (INT) 22

2.3.5 (E)-1,3,3-trimethyl-2-(2-(pyren-1-yl)vinyl)-3H-indol-1-ium (INP) 23

2.4 Studies of photophysical properties 24

2.4.1 Molar extinction coefficient (ε) 24

2.4.2 Relative quantum yield 24

2.5 Studies of selectivity and sensitivity 25

2.5.1 Anions selectivity 25

2.5.2 Anions interference 26

2.5.3 UV-Vis and fluorescence titration and Detection limit 26

2.6 Studies of sensing mechanism 26

2.6.1 Time dependent 26

2.6.2 ^{1}H-NMR experiment 27

2.6.3 Job's plot 27

2.7 Application of cyanide detection 27

2.7.1 Cyanide quantitative analysis in real water samples 27

2.7.2 Cyanide detection on paper-based support 27

CHAPTER III RESULT AND DISCUSSION 28

จุฬาลงกรณ์มหาวิทยาลัย
Chulalongkorn University

3.1 Synthesis and characterization of indolium-fluorophore conjugates (INJ, INT, INP)....28
3.2 Photophysical properties....30
3.3 Anions screening....31
3.4 Optimization condition....32
3.5 Selectivity toward cyanide....36
3.6 Sensitivity toward cyanide....42
3.7 Sensing mechanism....46
3.7.1 Job's plot....46
3.7.2 ^{1}H-NMR experiment....47
3.7.3 Mass spectrometry experiment....48
3.8 Utilization of indolium-fluorophore conjugates for cyanide detection....48
3.8.1 Quantitative analysis of cyanide in real water samples....48
3.8.2 Preliminary of paper-based....49
CHAPTER IV CONCLUSIONS....52
REFERENCES....53
APPENDIX....1
VITA....8

จุฬาลงกรณ์มหาวิทยาลัย
Chulalongkorn University

LIST OF TABLES

Page

Table 3.1 Photophysical properties of target molecules 31

Table 3.2 Performance of indolium fluorophore conjugates as a cyanide sensor.....45

Table 3.3 Quantitative analysis of CN^- in four types of water by using INT.....49

Table 3.4 Comparison sensitivity of CN^- fluorescence sensors.....51

จุฬาลงกรณ์มหาวิทยาลัย
CHULALONGKORN UNIVERSITY

LIST OF FIGURES

Page

Figure 1.1 Jablonski diagram describing photophysical processes 1

Figure 1.2 Mode of fluorescence responding..... 2

Figure 1.3 ICT process energy diagram..... 3

Figure 1.4 The proposed mechanism for the determination of CN^-, using probe at DMSO solution. 4

Figure 1.5 (a) Nucleophilic reaction between CN^- and cyanine dyes with indolium–coumarin linkages. (b) Fluorescent spectra (λex = 415 nm) of indolium–coumarin derivative, measured with 20 equiv. of each respective anion in a buffered water/MeCN mixture (7/3 v/v; CHES 100 mM, pH 9.0)..... 5

Figure 1.6 (a) Sensing mechanism for CN^- and HSO_3^- (b) Emission ratio I_{465}/I_{571} of 1 (10 μM) in PBS buffer (pH 7.4,10 mM) in the presence of various species. λ_{ex} = 400 nm: 1, probe alone; 2, HSO_3^-; 3, HS^-; 4,CN^-; 5, F^-; 6, Cl^-; 7, Br^-; 8, I^-; 9, AcO^-; 10, ClO_4^-; 11, NO_3^-; 12,N_3^-; 13, SO_4^{2-}; 14, HSO_4^-; 15, SCN^-; 16, PO_4^{3-}; 17, HPO_4^{3-}; 18,$H_2PO_4^{3-}$ (c) Photographs of the test paper exposure to various species under UV light (365 nm). . 6

Figure 1.7 The proposed mechanism for novel cyanide fluorescent sensor based on indolium after addition of cyanide..... 7

Figure 1.8 Fluorescence spectra of indolium derivative with increasing of cyanide concentration in water (40 μM, HEPES buffer, pH 7.4). and their possible reaction between probe and cyanide. 7

Figure 1.9 (a) UV–vis spectra of N1 (20 μM) in H_2O [0.01 M Tris-HCl buffer, pH 7.2] upon adding an increasing concentration of CN^-. (b) Fluorescence spectra of N1 upon adding an increasing concentration of CN^-..... 8

Figure 1.10 (a) Absorption spectra (b) Fluorescence spectra during CN^- concentration increased monitoring in Tris-HCl buffer, pH 7.2. 9

จุฬาลงกรณ์มหาวิทยาลัย
Chulalongkorn University

Figure 1.11 Changes in the absorbance and fluorescence intensities of PI when adding 2 equiv. of different anions. 10

Figure 1.12 Fluorescence spectra of julolidine–thiocarbonohydrazone 2 (10.0 mM) and on the addition of salts (20.0 equiv) of Li^{+}, Na^{+}, Ba^{2+}, Sr^{2+}, Mg^{2+}, Al^{3+}, Ca^{2+}, Mn^{2+}, Fe^{2+}, Co^{2+}, Ni^{2+}, Zn^{2+}, Ag^{+}, Cd^{2+}, Hg^{2+}, Pb^{2+}, and Cu^{2+} in aqueous medium (50 mM HEPES/MeCN, 6:4, v/v; pH 7.2). 11

Figure 1.13 Fluorescence spectra in the presence of different concentrations of Al^{3+} ions in bis-tris buffer solution (10 mM, pH 7.0). 12

Figure 1.14 Mechanism of HSO_3^{-}/SO_3^{2-} sensing by CQT.....12

Figure 1.15 Proposed binding mode of TPA-Th for the recognition of Cr^{3+}.....13

Figure 1.16 (a) UV–Vis spectra changes and (b) Emission spectra response of TPA-PTH (20 μM) over 10 equiv. of various cations in $CH_3CN:H_2O$ (7:3, v/v). 14

Figure 1.17 Fluorescent sensing mechanism between the TPAPI sensor with hydrazine. 15

Figure 1.18 The spectra of fluorescence and colorimetric change after increasing of hypochlorite concentration.....16

Figure 1.19 The fluorescence spectra of PBZ in the presence of various metal ions in EtOH-HEPES buffer (65:35, v/v, pH = 7.20) at 526 nm. 16

Figure 1.20 Selective fluorescence response of PAI under different metal ions in DMF. 17

Figure 1.21 Target molecules.....18

Figure 22 ^{1}H-NMR of INJ, INT and INP in DMSO-d6.....29

Figure 23 Normalized absorption and emission spectra of INJ, INT and INP in acetonitrile (10 μM). 31

Figure 24 Fluorescence selectivity screening of INJ, INT and INP toward 11 types of anions in acetonitrile. 32

จุฬาลงกรณ์มหาวิทยาลัย
Chulalongkorn University

Figure 25 (a) Fluorescence spectra of INJ after the addition of CN^- in various solvents (b) Fluorescence spectra of INJ after the addition of CN^- in various percentages of H_2O in acetonitrile. 33

Figure 26 (a) Fluorescence intensity plot of INJ (10 μM) in MilliQ water in the presence of Triton X-100 at various concentration, with CN^- (10 μM) and (b) Fluorescence intensity plot of INJ (10 μM) in aqueous buffer solution at various pHs, with and CN^- (10 μM). 35

Figure 27 Sensing time observation on fluorescence intensity of INJ, INT and INP monitoring in HEPES buffer pH 8.0 in the presence of 200 μM Triton X-100 with 10 μM of CN^-. 36

Figure 28 (a) Colorimetric selectivity of INJ, INT and INP toward 11 types of anions in HEPES buffer pH 8.0 with 200 μM Triton X-100, (b) Absorbance spectra of INJ with anions, (c) Absorbance spectra of INT with anions, (d) Absorbance spectra of INP with anions. 38

Figure 29 (a) Absorbance spectra of INJ upon increasing of CN^-, (b) Absorbance spectra of INT upon increasing of CN^-, (c) Absorbance spectra of INP upon increasing of CN^-. 39

Figure 30 (a) Fluorescence selectivity of INJ, INT and INP toward 11 types of anions in HEPES buffer pH 8.0 with 200 μM Triton X-100, (b) Fluorescence spectra of INJ with anions, (c) Fluorescence spectra of INT with anions, (d) Fluorescence spectra of INP with anions. 40

Figure 310 Interference test for INJ, INT and INP with CN^- 10 μM in the presence of other anions (100 μM) in HEPES buffer pH 8.0 with 200 μM Triton X-100 41

Figure 32 (a) Absorbance spectra of INJ during increased concentration of CN^- (b) Calibration Curve of INJ (c) Absorbance spectra of INT during increased concentration of CN^- (d) Calibration Curve of INT (e) Absorbance spectra of INP during increased concentration of CN^- (f) Calibration Curve of INP 43

จุฬาลงกรณ์มหาวิทยาลัย
Chulalongkorn University

Figure 33 (a) Fluorescence spectra of INJ during increased concentration of CN^- (b) Calibration Curve of INJ (c) Fluorescence spectra of INT during increased concentration of CN^- (d) Calibration Curve of INT (e) Fluorescence spectra of INP during increased concentration of CN^- (f) Calibration Curve of INP 45

Figure 34 (a) Job's plot from fluorescence intensities of INJ with mole fraction CN- monitoring at 403 nm, (b) Job's plot from fluorescence intensities of INT mole fraction with CN^- monitoring at 412 nm and (c) Job's plot from fluorescence intensities of INP with CN^- monitoring at 491 nm. 46

Figure 35 ^{1}H-NMR of INT before and after the addition of CN^- 0.5 and 1 equivalent monitoring in DMSO-d6. 47

Figure 36 DART-TOF Mass spectrum of INT-CN adduct. 48

Figure 37 (a) INJ 10 mM on paper-based support with four different CN^- concentration (10 µL each) (b) INT 1 mM on paper-based support with four different CN^- concentration (10 µL each) 50

Figure 38 ^{1}H-NMR spectrum of 1,2,3,3-Tetramethyl-3H-indolium iodide in $CDCl_3$ 1

Figure 39 HRMS spectrum of 1,2,3,3-Tetramethyl-3H-indolium iodide 1

Figure 40 ^{1}H-NMR spectrum of INJ in DMSO-d6 2

Figure 41 ^{13}C-NMR spectrum of INJ in DMSO-d6 2

Figure 42 HRMS spectrum of INJ 3

Figure 43 ^{1}H-NMR spectrum of 4-(diphenylamino) benzaldehyde in $CDCl_3$ 3

Figure 44 ^{1}H-NMR spectrum of INT in DMSO-d6 4

Figure 45 ^{13}C-NMR spectrum of INT in DMSO-d6 4

Figure 46 DART-TOF MS spectrum of INT 5

Figure 47 ^{1}H-NMR spectrum of INP in DMSO-d6 5

Figure 48 ^{13}C-NMR spectrum of INP in DMSO-d6 6

Figure 49 DART-TOF MS spectrum of INP 6

จุฬาลงกรณ์มหาวิทยาลัย
Chulalongkorn University

Figure 50 ^{1}H-^{1}H COSY NMR spectrum of INT 1: CN 0.5 in DMSO-d6 7

Figure 51 ^{13}C-NMR spectrum of INT-CN adduct in DMSO-d6 7

จุฬาลงกรณ์มหาวิทยาลัย
CHULALONGKORN UNIVERSITY

CHAPTER I

INTRODUCTION

1.1 Fluorescence

The fluorescence phenomenon is the one of radiative process in the consequence of energy releasing from excited molecules that basically described by the Jablonski diagram (**Figure 1.1**) [1, 2]. When the organic molecules absorb light with a suitable energy, molecule will be activated from ground state (S_0) to the higher electronics state (S_1 or S_2 or higher). The excited molecules which is not stable will rapidly release some energy in term of thermal or kinetics energy then settle in the lowest electronics level of the first excited state (S_1). This process is geometrically relaxation which occur via vibration and rotation without emitting light. The remaining energy in molecules will be released as the fluorescence light and the molecules return directly back from S_1 to the ground state S_0. The fluorescence lifetime usually consumes in nano-second. The degree of relaxation implies the difference of absorption and emission wavelength which can refer to fluorophore characteristic.

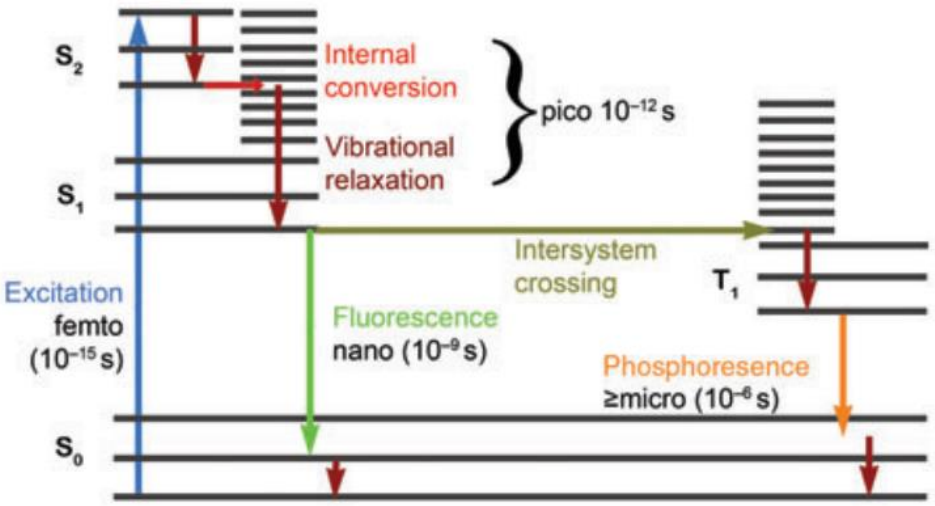

Figure 1.1 Jablonski diagram describing photophysical processes

1.2 Fluorescence sensor

In the past decade, fluorescence sensor is a versatile tool for the analyte recognition, resulting various publications reported their performance toward numerous types of target molecules such as metal ions, anions, and biological molecules [3]. In comparison to other analytical methods, fluorescence technique willing to provide an accuracy result, high sensitivity toward the analyte, and lower cost of equipment. Interestingly, portable device such as paper-based strip can be applied with fluorescent sensors for convenient on-site analysis. Basically, fluorescence sensor consists of two main components which are receptor unit, specific binding site for the analyte, and signaling unit, expressing the fluorescence signal. The responding mode of fluorescence sensor express as the changing in fluorescence emission which could be turn-on, turn-off, or wavelength shift as shown in **Figure 1.2**.

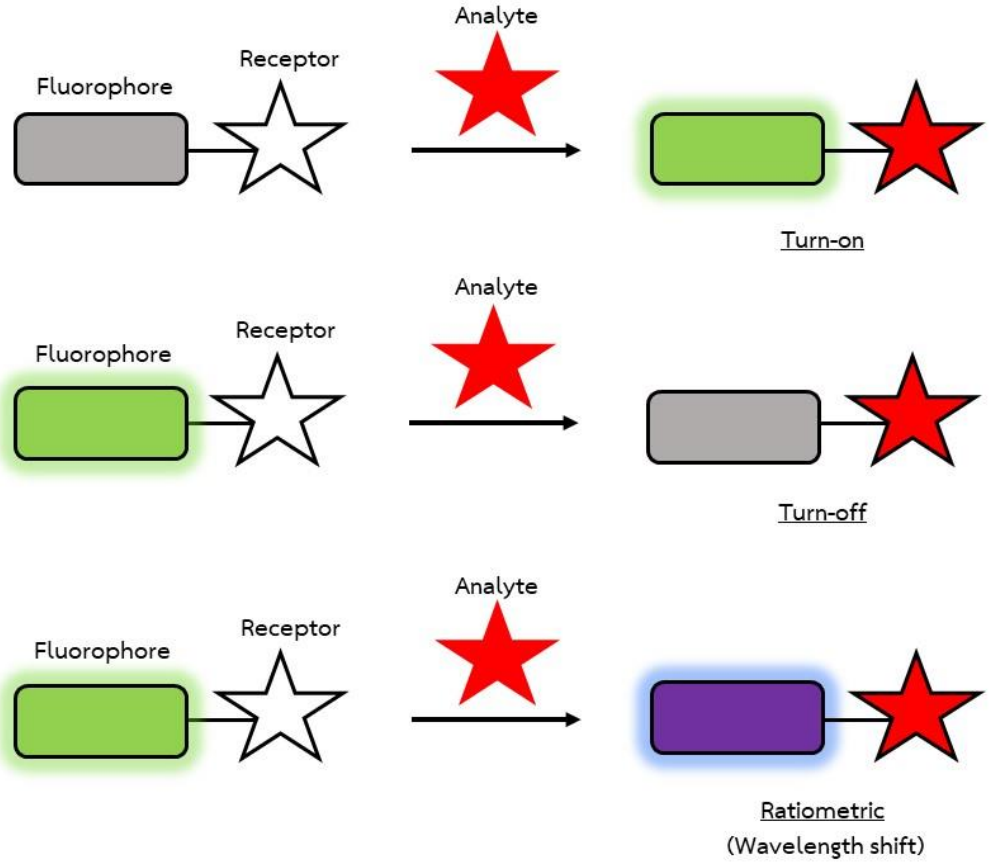

Figure 1.2 Mode of fluorescence responding.

1.3 Sensing Mechanism

The interaction between analyte and receptor provides many photophysical signaling mechanisms including the photoinduced electron transfer (PET) [4-7], fluorescence resonance energy transfer (FRET) [8-10], Intermolecular charge transfer (ICT) [11-13], excited-state intramolecular proton transfer (ESIPT) [14-16], aggregation induced enhancement fluorescence (AIE) [17-19], and excimer formation [20, 21]. In the rational design for fluorescence sensors, it normally focuses on one or more than one sensing mechanism which related to the characteristic of corresponding fluorophore to adjust their selectivity and sensitivity. In this research, the designed compounds will be mainly involved in ICT process.

- Intermolecular charge transfer (ICT)

  The molecule in local excited state (most stable excited state of S_1) could undergo the geometrical relaxation which relocated the electron cloud. This phenomenon usually occurs when the electron donor and electron acceptor connect via π conjugation. The new lower excited state would be generated as internal charge transfer (ICT). The molecule at ICT state could relax to the ground state and release the light that settle within or out of visible region [22]. The fluorescence sensor could be designed by employ this ICT process principle.

จุฬาลงกรณ์มหาวิทยาลัย

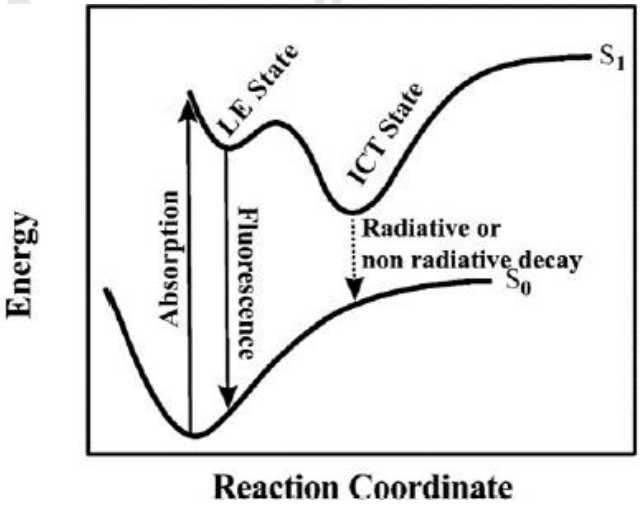

Figure 1.3 ICT process energy diagram

1.4 Literature reviews

1.4.1 Fluorescence sensor based on Indolium unit for cyanide detection

Among a huge number of fluorescence receptors, there are many reports suggest that the structure of indolium moiety could be an effective receptor unit for cyanide analysis [23-26]. The conjugation between indolium and fluorescence fluorophore usually bring a selective detection toward anions through the nucleophilic addition reaction especially cyanide ion. Their sensitivity, selectivity and photophysical properties can be adjusted and improved by varying their signaling component.

In 2014, Yang and coworker reported the turn-on fluorescence probe based on indolium structure which is highly selective on cyanide (**Figure 1.4**)[27]. Blue-green fluorescence was appeared gradually upon CN^- adding. The fluorescence turn-on was induced by mechanism of nucleophilic addition reaction after cyanide ion attacking onto indolium group since; the attack of anion blocked their **π**-electron conjugation. The compound exposes a good limit of detection around 45 nM in DMSO solution system. Furthermore, the adduct between synthesized probe and cyanide was confirm by using ^{1}H-NMR and mass spectrometry.

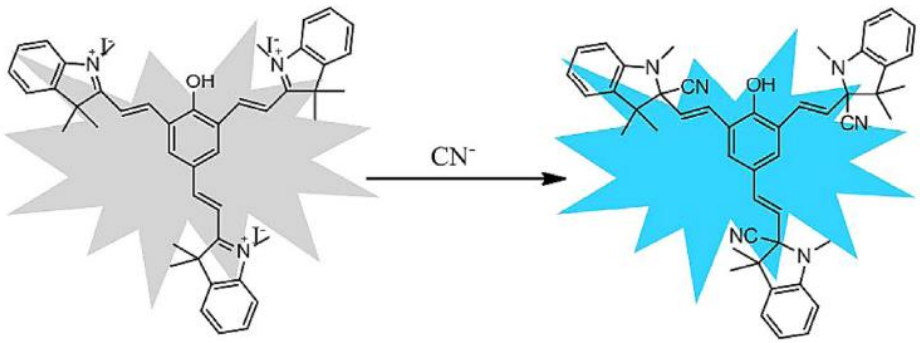

Figure 1.4 The proposed mechanism for the determination of CN^-, using probe at DMSO solution.

In similarly, shiraishi group also designed cyanine dyes via the conjugation between indolium and coumarin derivatives [28]. The nucleophilic addition of CN^- create strong aqua blue fluorescence due to the suppression of ICT process accommodating delocalization of electron on coumarin component. Synthesized

indolium-coumarin derivatives expressed the excellent fluorescence selectivity toward only cyanide ion in water/MeCN solvent system (**Figure 1.5**). The sensitivity toward CN^- is appeared to be quite moderate with detection limit in the range of 0.4-0.5 μM. Interestingly, chlorine atom contained derivative showed the faster sensing time comparison to others with the higher binding constant in the result of inductive effect which increased the electrophilicity of indolium active site.

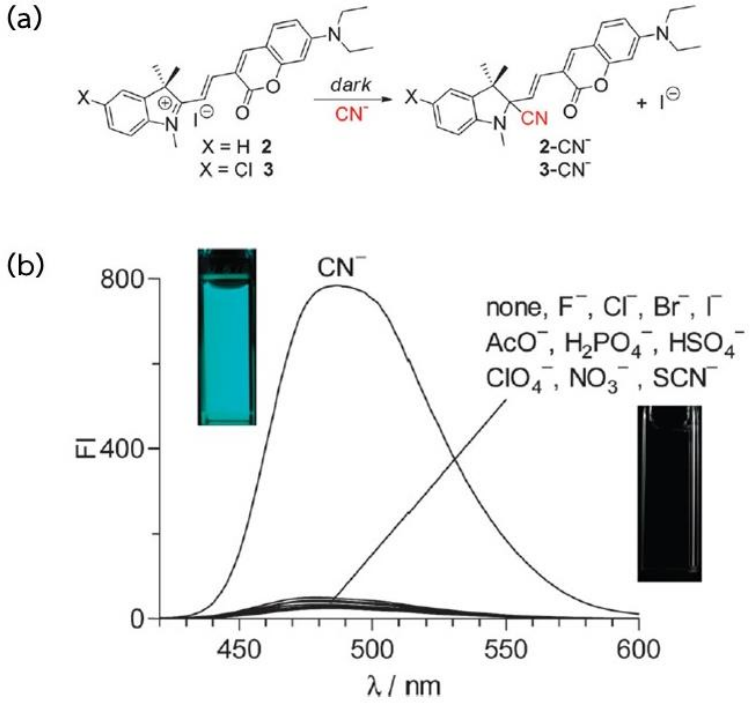

Figure 1.5 (a) Nucleophilic reaction between CN^- and cyanine dyes with indolium–coumarin linkages. (b) Fluorescent spectra (**λ**ex = 415 nm) of indolium–coumarin derivative, measured with 20 equiv. of each respective anion in a buffered water/MeCN mixture (7/3 v/v; CHES 100 mM, pH 9.0)

CHULALONGKORN UNIVERSITY

During the same period, Sun et al. prepared indolium moiety as a cyanide and bisulfite recognition unit by one step synthesis [29]. The nucleophilic addition of cyanide took place on 1,2 positions of structure in pH above 9.0 while, the 1,4 additions of HSO_3^- underwent smoothly in aqueous solution (pH 7.4) on the structure showing in **Figure 1.6a** resulting both colorimetric and fluorescent color change.

This probe showed strong selectivity toward bisulfite ion in PBS buffer solution pH 7.4 with short response time. They further observed preliminary paper test strip

system which included CN^- and HS^-, well known targeted anions for indolium moiety. The result revealed clear color change that could be easily distinguished as shown in **Figure 1.6c**. To confirm the utilization of this fluorescence probe, sugar samples which is containing bisulfite moiety was investigated in this literature.

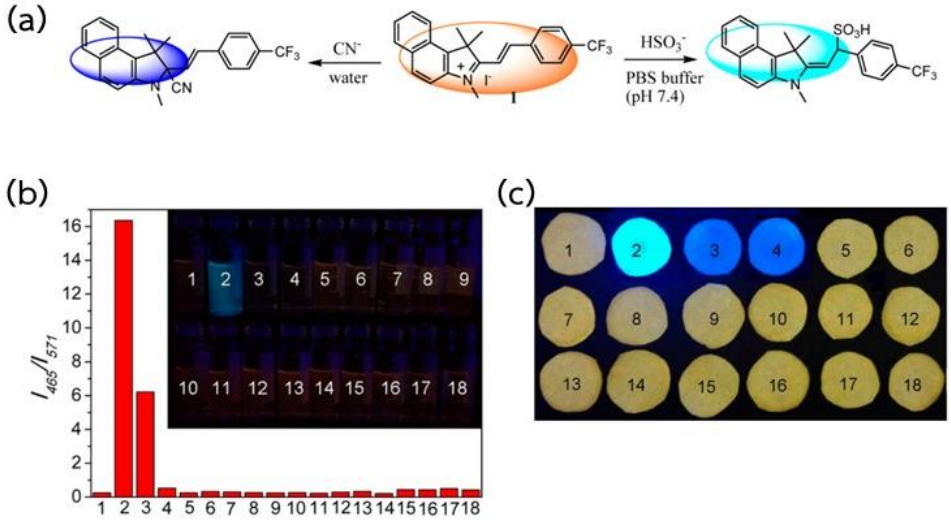

Figure 1.6 (a) Sensing mechanism for CN^- and HSO_3^- (b) Emission ratio I_{465}/I_{571} of **1** (10 μM) in PBS buffer (pH 7.4,10 mM) in the presence of various species. λ_{ex} = 400 nm: 1, probe alone; 2, HSO_3^-; 3, HS^-; 4,CN^-; 5, F^-; 6, Cl^-; 7, Br^-; 8, I^-; 9, AcO^-; 10, ClO_4^-; 11, NO_3^-; 12,N_3^-; 13, SO_4^{2-}; 14, HSO_4^-; 15, SCN^-; 16, PO_4^{3-}; 17, HPO_4^{3-}; 18,$H_2PO_4^{3-}$ (c) Photographs of the test paper exposure to various species under UV light (365 nm).

จุฬาลงกรณ์มหาวิทยาลัย
Chulalongkorn University

In 2017, novel cyanide fluorescent sensor was developed in our laboratory by Promchat and coworkers as shown in **Figure 1.7** [25]. The synthesized derivative showed strong selectivity toward cyanide over other anions on both colorimetric and fluorometric mode. The sensitivity for their colorimetric observed was report as 1.9 μM in HEPES buffer pH 6.0 with Triton X-100 (220 μM). On the other hands, fluorescence method provided the higher sensitivity at the detection limit of 49 nM. Interestingly, this research suggested that the sonication could increase the solubility of compound which led to the increasing in sensitivity to 0.54 nM which were incredibly sensitive.

Figure 1.7 The proposed mechanism for novel cyanide fluorescent sensor based on indolium after addition of cyanide.

Another turn-on fluorescent probe based on indolium unit was reported by Liu and coworker in 2018 [30]. As expected, among 13 anions, Indolium conjugated with triphenylimidazole moiety selectively underwent 1,2 additions toward CN^- in aqueous solution (**Figure 1.8**). The obvious fluorescence change is occurred to give blue color under black light and show the excellent sensitivity with 20nM of LOD. The colorimetric change, solution color faded, also clearly observed by naked eye. Water samples were used for real CN^- investigation to confirm the advantages of their performance in water of the synthesized molecule revealing a good recovery of found cyanide. Furthermore, this fluorescence probe could be applied in the living cell that incubating with CN^-.

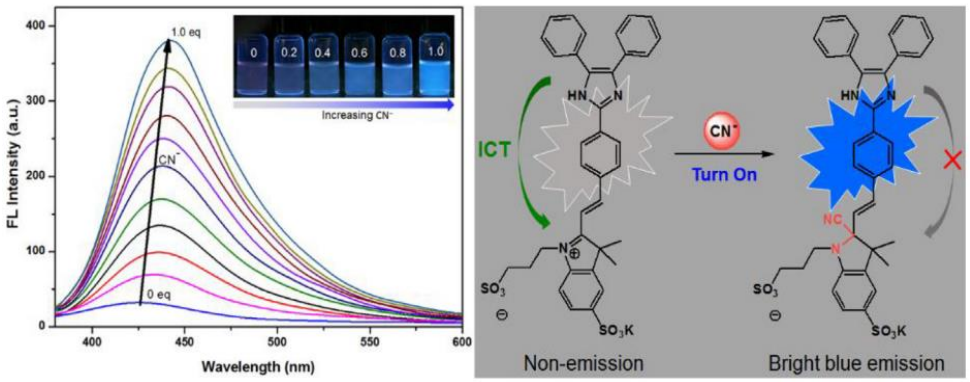

Figure 1.8 Fluorescence spectra of indolium derivative with increasing of cyanide concentration in water (40 μM, HEPES buffer, pH 7.4). and their possible reaction between probe and cyanide.

Most of indolium conjugation compounds responded toward cyanide ion via turn-on fluorescence, however, there are some reports provided the study related to turn off fluorescence mechanism between cyanide and indolium receptor.

One of turn-off fluorescence sensors based on indolium unit were developed in 2019, Li and coworker prepared dimethylaminobenzene conjugated with indolium component [31]. The selectivity of compound **N1** against cyanide was investigated on both colorimetric and fluorescence measurement as shown in **Figure 1.9**. Bleaching solution observed under room light bringing significant decreasing in fluorescence signal with the low detection limit (33.4 nM) in buffer pH 7.2 indicated an excellent detection activity. They further studied the sensing mechanism of compound by using ^{1}H-NMR revealing the upfield shifted of peak in the result of indolium's positive charge disappeared.

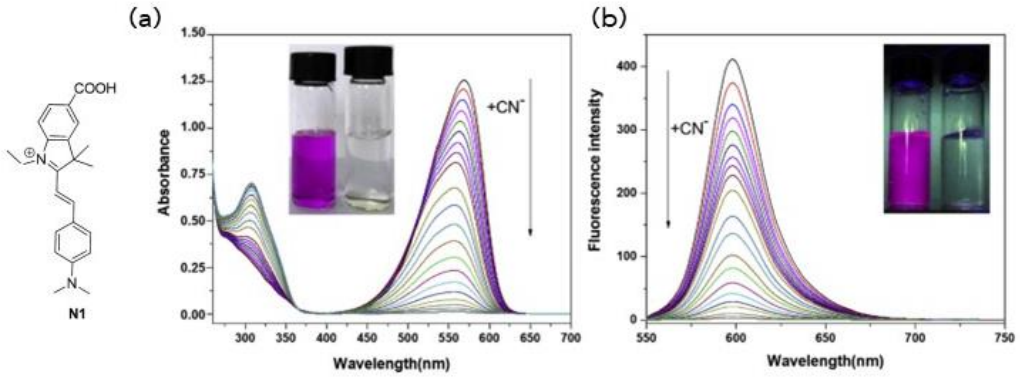

Figure 1.9 (a) UV–vis spectra of **N1** (20 μM) in H_2O [0.01 M Tris-HCl buffer, pH 7.2] upon adding an increasing concentration of CN^-. (b) Fluorescence spectra of **N1** upon adding an increasing concentration of CN^-

จุฬาลงกรณ์มหาวิทยาลัย
CHULALONGKORN UNIVERSITY

In the same manner, in 2020, group of Cheng reported the investigation of another carboxylic indolinium structure conjugated with a coumarin component which exhibited the quenching of fluorescence signal, while colorimeric change could be noticed by naked eye during the cyanide concentration increasing as shown in **Figure 1.10** [32]. The detection limit was illustrated at 4.4 nM in Tris-HCl buffer, pH 7.2. This compound provided low cell cytotoxicity.

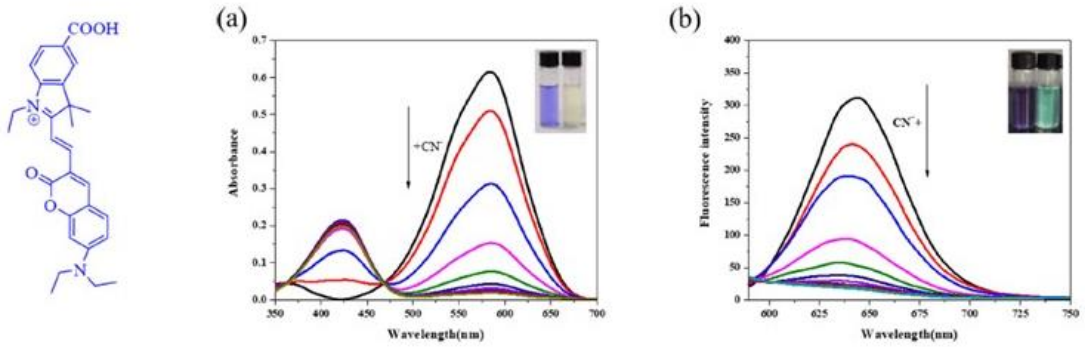

Figure 1.10 (a) Absorption spectra (b) Fluorescence spectra during CN^- concentration increased monitoring in Tris-HCl buffer, pH 7.2.

Recently, Phenothiazine-indolium derivatives was synthesized by Morikawa et. Al [33]. The selectivity against cyanide ion could be observed on both colorimetric and fluorescence as expected. Interestingly, sulfide ion also had ability to bind with the indolium derivatives yielding color of solution changing upon sulfide concentration increasing (**Figure 1.11**). With the small binding constant of sulfide ion toward fluorescence probe, the phenothiazine-indolium derivatives was specific toward only cyanide ion in term of fluorescence.

จุฬาลงกรณ์มหาวิทยาลัย
CHULALONGKORN UNIVERSITY

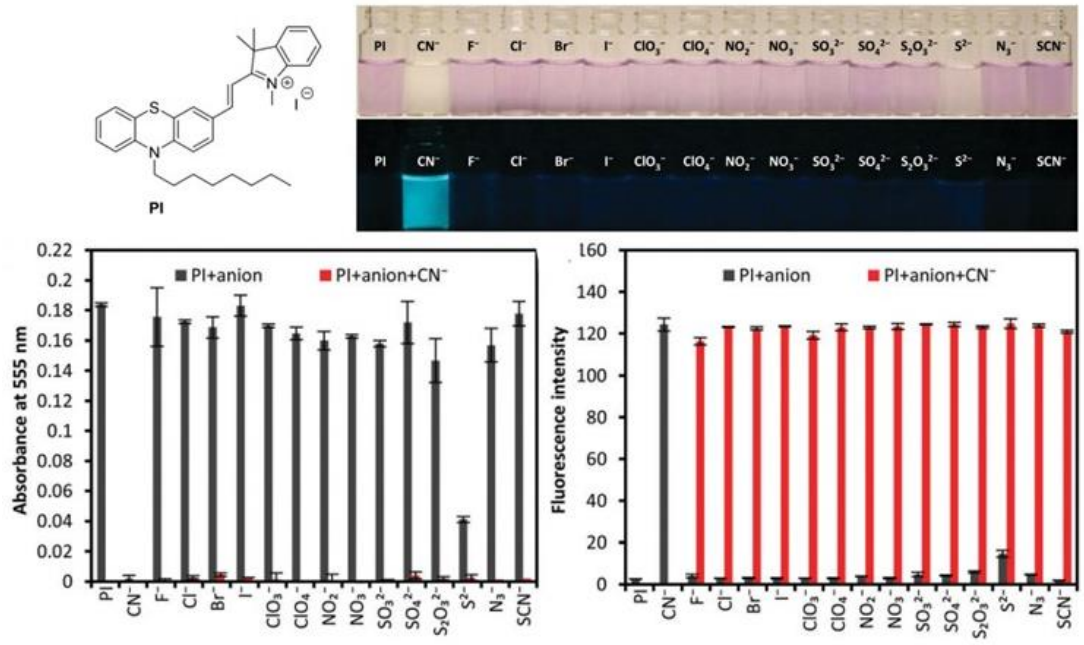

Figure 1.11 Changes in the absorbance and fluorescence intensities of **PI** when adding 2 equiv. of different anions.

1.4.2 Signaling unit for fluorescence sensor

- Julolidine

Julolidine is the N-containing compound which generally exhibited strong fluorescence with high quantum yield that could increase the sensitivity of designed fluorescence sensors [34-38].

Utilization of julolidine moiety within fluorescence field always develop in past decade, in 2011, group of Maity presented the julolidine contained fluorescent chemosensor with turn-off fluorescence mechanism (**Figure 1.12**) [39]. The designed julolidine **1** and **2** express the strong selectivity toward Cu^{2+}. In the case of **1**, the colorimetric change obliviously discovered but there is no any fluorescence response. On the other hands, compound **2** showed the turn-off fluorescence during cyanide incubation. The fluorescence signal could be recovered by adding of EDTA.

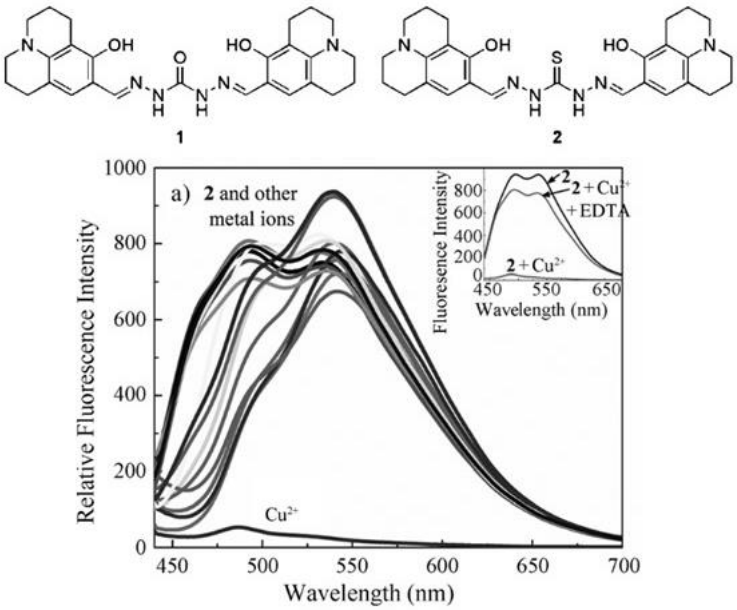

Figure 1.12 Fluorescence spectra of julolidine–thiocarbonohydrazone **2** (10.0 mM) and on the addition of salts (20.0 equiv) of Li^{+}, Na^{+}, Ba^{2+}, Sr^{2+}, Mg^{2+}, Al^{3+}, Ca^{2+}, Mn^{2+}, Fe^{2+}, Co^{2+}, Ni^{2+}, Zn^{2+}, Ag^{+}, Cd^{2+}, Hg^{2+}, Pb^{2+}, and Cu^{2+} in aqueous medium (50 mM HEPES/MeCN, 6:4, v/v; pH 7.2).

Another derivative of hydroxy julolidine was reported by group of Choi in 2016 as a fluorescent chemosensor for Al^{3+} [40]. Julolidine-tryptophan composite displayed significant selectivity against Al^{3+} over other metals (**Figure 1.13**). Fluorescence titration of Al^{3+} reveal the detection limit in the level of 6.4 μM in bis-tris buffer solution which is lower than the concentration mentioned in WHO guidance. Moreover, the biocompatibility of the complex was examined in the living cells. It turned to be low toxicities which indicated that the compound could be applied for bioimaging application.

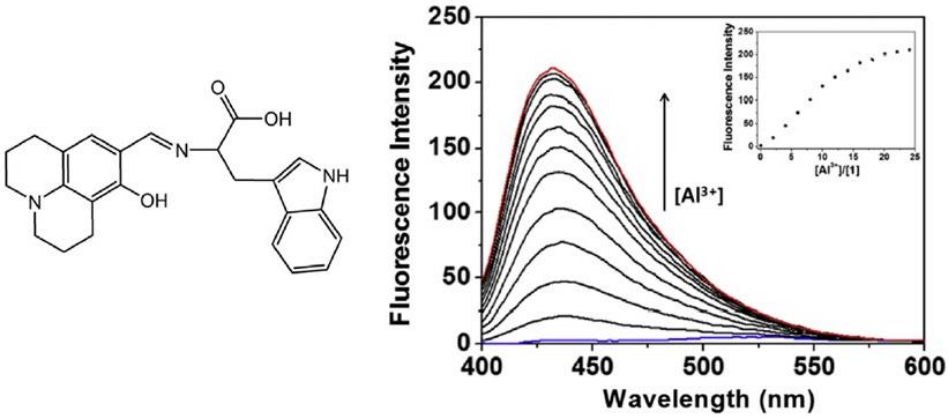

Figure 1.13 Fluorescence spectra in the presence of different concentrations of Al^{3+} ions in bis-tris buffer solution (10 mM, pH 7.0).

In recent year, a coumarin-quinoline-julolidine molecular system was developed by Liu and coworker for using as a HSO_3^- /SO_3^{2-} detector as shown in **Figure 1.14** [41]. Synthesized compound (**CQT**) responded toward analyte selectively on both colorimetric and fluorescence measurement in PBS buffer solution (pH = 7.4, 0.5 mM Triton X-100, containing 50% DMSO). Michael addition of HSO_3^- onto **CQT** brought blue fluorescence signal due to blocking of FRET process. The detection limit exhibited around 2.8 μM which could be applied for SO_2 derivatives quantitative analysis.

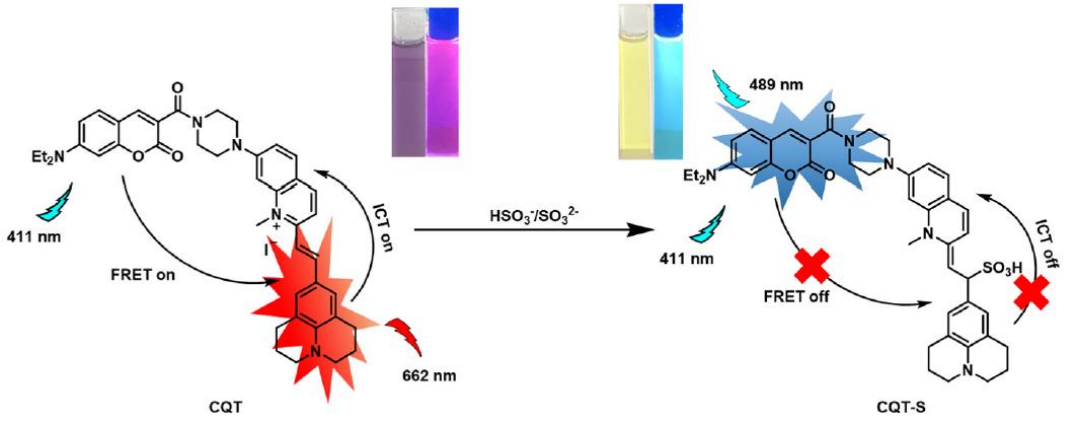

Figure 1.14 Mechanism of HSO_3^-/SO_3^{2-} sensing by CQT.

- Triphenylamine

Triphenylamine is one of outstanding electron donating structure which usually involved in fluorescence sensor application [42-45]. Interesting point, triphenylamine could exhibited the aggregation-induced emission (AIE) bringing the stronger fluorescence signal in many cases [19, 44, 46, 47].

In 2020, Kolcu and coworker synthesized derivative of triphenylamine with thiophene conjugation [48]. Turn-on fluorescence response was observed during addition of Cr^{3+} into solution of **TPA-Th** since the PET process was prohibited. The presented of N and S atoms on core structure serve as a suitable binding site for Cr^{3+} (**Figure 1.15**). The selectivity toward Cr^{3+} could be observed on both colorimetric and fluorescence and the sensitivity of sensor in fluorescence mode was calculated to be 1.5 μM in THF/H_2O (1:1).

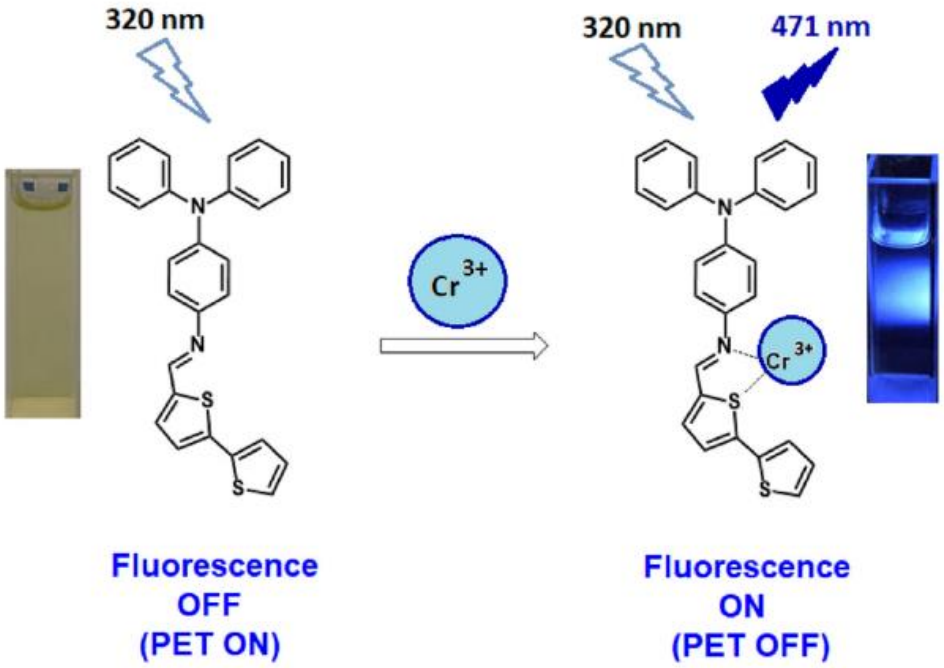

Figure 1.15 Proposed binding mode of **TPA-Th** for the recognition of Cr^{3+}.

On the other hands, Fluorescence sensor which contains triphenylamine and sulfone moiety was reported by Mohanasundaram and coworkers in 2022 [49]. The synthesized sensor presented the turn off fluorescence with strong selectivity against Cu^{2+} monitoring in MeCN/H_2O mixture solution (**Figure 1.16**). The

concentration ratio from Job's plot indicated that this sensor binds to Cu^{2+} with 2:1 ratio. This compound showed the detection limit at 12.5 nM.

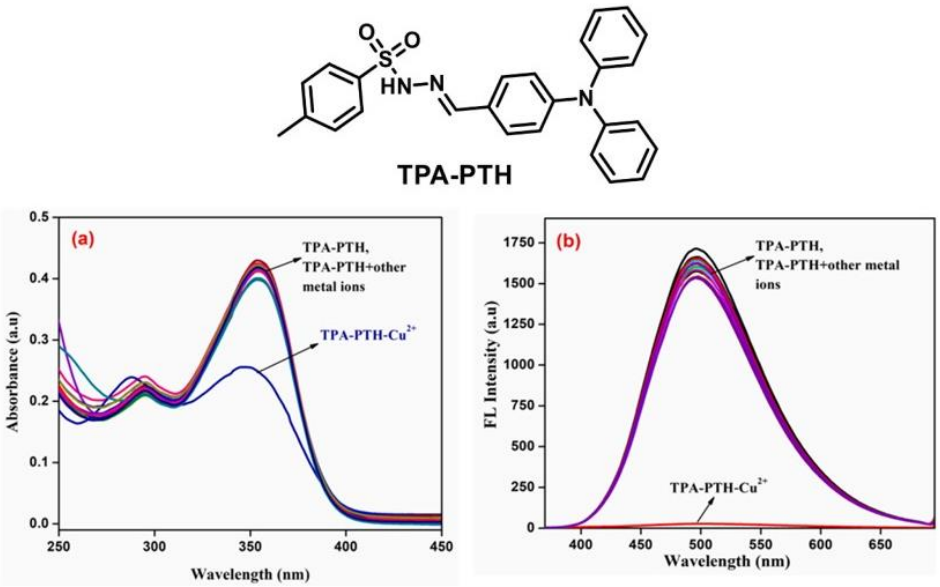

Figure 1.16 (a) UV–Vis spectra changes and (b) Emission spectra response of TPA-PTH (20 μM) over 10 equiv. of various cations in CH_3CN:H_2O (7:3, v/v).

Recently, Group of Li reported the triphenylamine-based fluorescence sensor (**TPAPI**) for hydrazine detection in water [50]. **TPAPI** showed aggregation induced emission (AIE) in solid state leading a strong red fluorescence. Since, **TPAPI** had a poor solubility in water, when the solvent system contains water more than 60%, red fluorescence was clearly detected. The fluorescence decreased gradually during hydrazine addition. Interestingly, 10% water as a media system gave the different mode of detection. There was originally no fluorescence observed in 10% water then fluorescence becoming up after hydrazine uptake as result of aggregation caused quenching (ACQ) (**Figure 1.17**). The sensitivity of this compound was calculated to be 137 nM. Moreover, paper test strip for hydrazine detection was prepared successfully from this sensor.

จุฬาลงกรณ์มหาวิทยาลัย
Chulalongkorn University

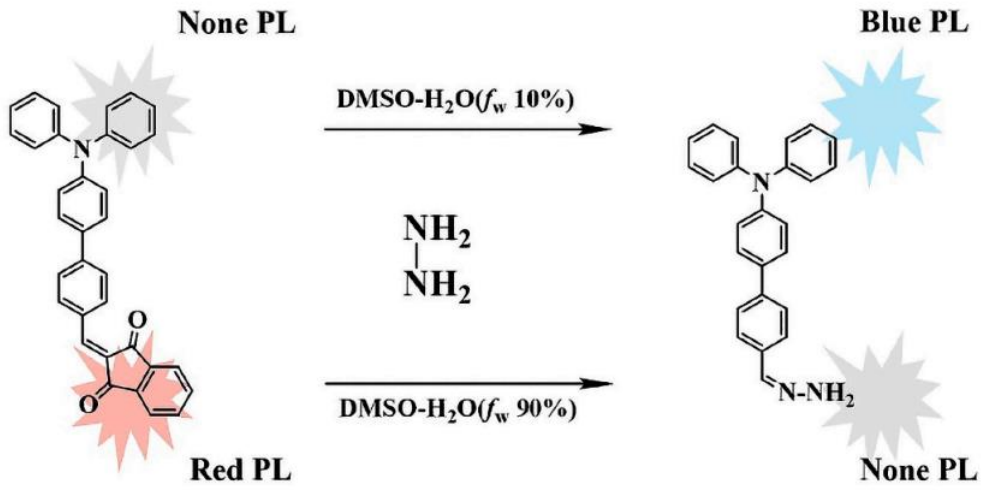

Figure 1.17 Fluorescent sensing mechanism between the **TPAPI** sensor with hydrazine.

- Pyrene

It's been a long time that pyrene unit was defined to be a classical and famous fluorophore in the fluorescence sensor field with their exceptional characteristic such as high quantum yield and excimer formation [51-55]. Pyrene excimer was expected to enhance the fluorescence. Variety of pyrene derivatives were applied as a fluorescence sensor for various target molecule.

In 2015, Zang et al. developed the pyrene containing fluorescence sensor for hypochlorite detection [56]. The synthesized compound was originally non-fluorescent because the conjugation of phenylhydra-zone group has a strong quenching effect on pyrene by PET process. The pyrene derivative displayed turn-on fluorescence and also colorimetric changed selectively toward hypochlorite in buffer pH 9.18/ethanol 1:4 v/v as shown in **Figure 1.18**. This could be a result of selective oxidation on phenylhydrazone unit by hypochlorite, which lead to the cleavage of the phenylhydrazone group and PET process prohibited.

จุฬาลงกรณ์มหาวิทยาลัย
Chulalongkorn University

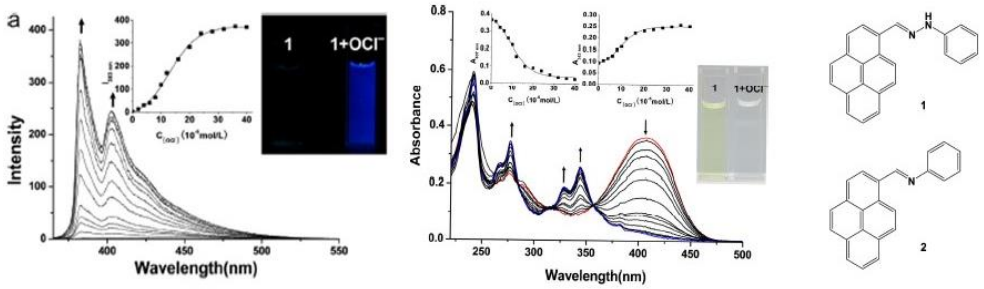

Figure 1.18 The spectra of fluorescence and colorimetric change after increasing of hypochlorite concentration.

Pyrene-based fluorescence sensor containing benzothiazole moiety was synthesized by group of Tang for the recognition of Zn^{2+} [57]. The turn on fluorescence significantly occurred after adding of Zn^{2+} in consequence of PET process was interrupted (**Figure 1.19**). The detection limit of this compound was carried out in EtOH-HEPES buffer (65:35, v/v, pH = 7.20) to be 258 nM. Job's plot, ^{1}H-NMR and ESI mass spectrometry were used to confirm the binding configuration between pyrene-based fluorescence and Zn^{2+}. Moreover, real water samples and bio-imaging in live cells were demonstrated to study their potential ability to recognize Zn^{2+}.

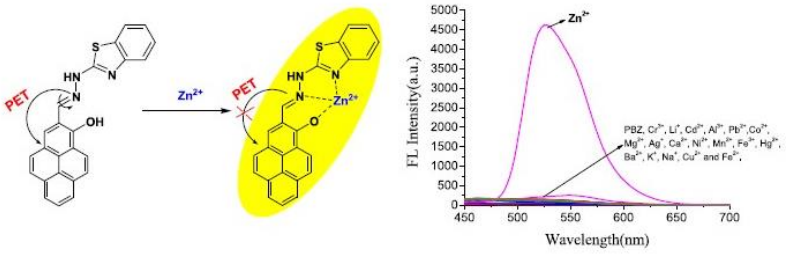

Figure 1.19 The fluorescence spectra of **PBZ** in the presence of various metal ions in EtOH-HEPES buffer (65:35, v/v, pH = 7.20) at 526 nm.

Recently, pyrene-based fluorescent probe for Al^{3+} detection was reported by Liu and coworkers [58]. This probe bearing 5-((pyren-1-ylmethylene) amino) isophthalate which proceed photoinduced electron transfer (PET) process so the compound showed non-fluorescence properties.

Addition of Al^{3+} would be cut C=N bond and expressed as the turn on fluorescence mechanism. Their detection limit was found to be 30.7 nM in DMF as shown in **Figure 1.20**.

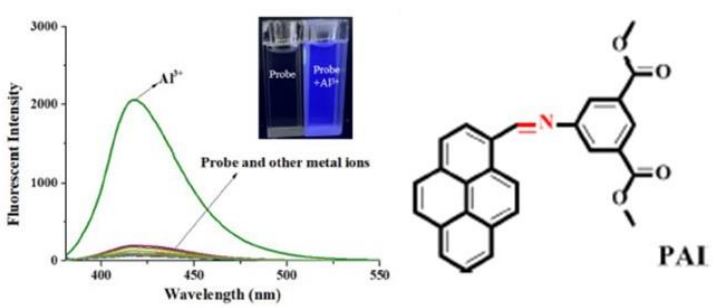

Figure 1.20 Selective fluorescence response of PAI under different metal ions in DMF.

All of the literatures mentioned above, the fluorescence sensor from indolium unit would be one of powerful method for cyanide detection. Their selectivity expected to be consistent toward cyanide by using indolium as a receptor and their sensitivity would be adjusted and improved through the varying of three outstanding fluorophores.

1.5 Objectives of this research

Here in, three indolium-fluorophore conjugates (**INJ**, **INT**, **INP**) (**Figure 1.21**) were developed in the objective to utilize as a fluorescence sensor for cyanide ion detection. Designed compounds contain indolium moiety as a recognition unit for cyanide and julolidine, triphenylamine, and pyrene are served as sensing unit. The different fluorophores are varying in expected to observe and comparison on their photophysical properties and cyanide detection performance in aqueous systems. Water samples from four different sources would be investigated for cyanide in real sample detection. Moreover, the preliminary result of the on-site analysis is also validated.

จุฬาลงกรณ์มหาวิทยาลัย
CHULALONGKORN UNIVERSITY

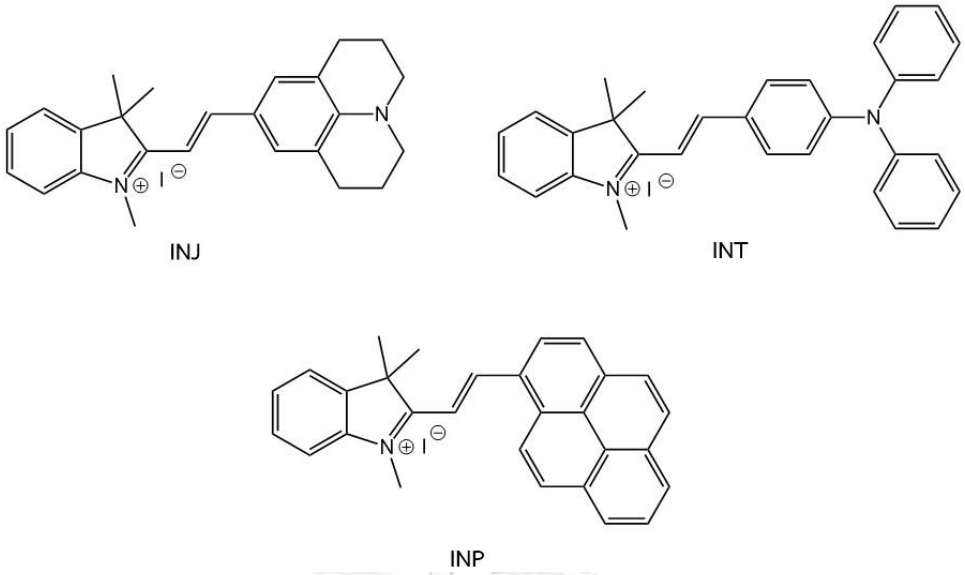

Figure 1.21 Target molecules.

จุฬาลงกรณ์มหาวิทยาลัย
Chulalongkorn University

CHAPTER II

EXPERIMENTAL

2.1 Reagents and materials

All reagents were purchased from Merck and Sigma-Aldrich. For most reactions, solvents such as methylene chloride (CH_2Cl_2) and methanol (MeOH) were reagent grade stored over molecular sieves. Solvents used for extraction and chromatography such as CH_2Cl_2, hexane, EtOAc and MeOH were commercial grade. Column chromatography was operated using Merck silica gel 60 (70-230 mesh) and Sigma Aldrich Sephadex G-25. Thin layer chromatography (TLC) was performed on silica gel plates (Merck F245). Milli-Q water was used in all experiments unless specified otherwise. The stock solutions of the 3 compounds, (E)-2-(2-(1,2,3,5,6,7-hexahydropyrido[3,2,1-ij]quinolin-9-yl)vinyl)-1,3,3-trimethyl-3H-indol-1-ium (**INJ**), (E)-2-(4-(diphenylamino)styryl)-1,3,3-trimethyl-3H-indol-1-ium (**INT**) and (E)-1,3,3-trimethyl-2-(2-(pyren-1-yl)vinyl)-3H-indol-1-ium (**INP**), were prepared at 1 mM and 10 mM in acetonitrile (CH_3CN) that were used as fluorescent probe in photophysical properties studies.

จุฬาลงกรณ์มหาวิทยาลัย
Chulalongkorn University

2.2 Methods

2.2.1 UV-Visible spectroscopy

The stock solutions of indolium-fluorophore conjugates were prepared with a concentration of 1.0 mM and 10 mM. The UV-Visible absorption spectra of the stock solutions of indolium-fluorophores conjugates were recorded from 200 to 600 nm at ambient temperature from a UV-2250 UV–vis spectrophotometer (SHIMADZU).

2.2.2 Fluorescence spectroscopy

The stock solutions of indolium-fluorophores conjugates were prepared with a concentration of 1.0 mM and 10.0 mM. The fluorescence spectra of the solutions of indolium-fluorophores were recorded from 200 to 600 nm at ambient temperature from a Carry Eclipse fluorescence spectrophotometer (Agilent Technologies).

2.2.3 ^{1}H and ^{13}C spectroscopy

^{1}H- and ^{13}C-NMR spectra were acquired from sample solution in $CDCl_3$ and DMSO-d_6 on Varian Mercury NMR spectrometer at 400 MHz, Bruker NMR spectrometer (ADVANCE III HD/Ascend 400 WB) at 400 MHz and JEOL NMR spectrometer (JNM-ECZ500R/S1) at 500 MHz for ^{1}H-NMR and 150 MHz for ^{13}C-NMR.

2.2.4 Mass spectroscopy

High-resolution mass spectra were carried out by MicroTOF-QII (Bruker company) with Dionex Ultimate (Thermo). Dart-TOF mass spectra were carried out by Dart-TOF JEOL mass spectrometer (JMS-T100LP)

จุฬาลงกรณ์มหาวิทยาลัย
Chulalongkorn University

2.3 Synthesis and characterization

2.3.1 1,2,3,3-Tetramethyl-3H-indolium iodide

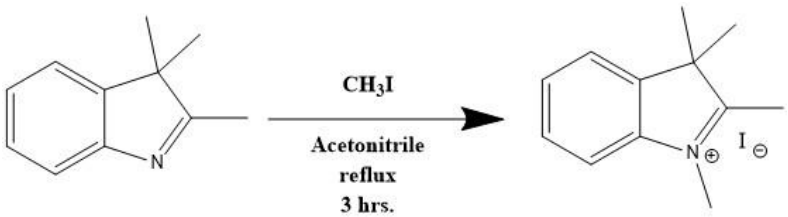

2,3,3-trimethyl-3H-indole (0.100 g, 0.628 mmol) was dissolved in acetonitrile (5mL). Methyl iodide (0.19 mL, 3.14 mmol) was added into the flask then refluxed for

3 hours, pink solid was obtained in 87% yield after purification by silica gel column chromatography using gradient hexane/ethyl acetate as an eluent. ^{1}H NMR (500 MHz, DMSO- D6) δ 7.67-7.59 (m, 4H), 4.30 (s, 3H), 3.14 (s, 3H), 1.71 (s, 6H). HRMS m/z: founded 174.12855 (calcd for $C_{12}H_{16}N_1^+$: 174.1282).

2.3.2 (E)-2-(2-(1,2,3,5,6,7-hexahydropyrido[3,2,1-ij]quinolin-9-yl)vinyl)-1,3,3-trimethyl-3H-indol-1-ium (**INJ**)

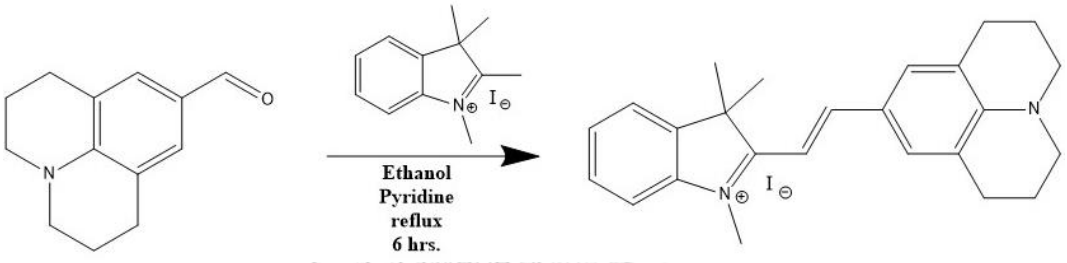

1,2,3,3-Tetramethyl-3H-indolium iodide (0.100 g, 0.332 mmol) and julolidine-1-carbaldehyde (0.067 g, 0.332 mmol) was mixed and dissolved in ethanol (5mL). Pyridine (0.04 mL, 0.498 mmol) was gently added into the flask then refluxed for 5 hours. The reaction was cooled down and evaporated then the precipitation was performed in ethyl acetate/hexane. The crude product was purified by Sephadex G-25 column chromatography using MeOH/CH_2Cl_2 1: 2 (v/v) as an eluent. Violet solid was obtained in 93% yield after purification. ^{1}H NMR (500 MHz, DMSO-D6) δ 8.13 (d, J = 15.4 Hz, 1H), 7.74 – 7.64 (m, 3H), 7.61 (d, J = 7.7 Hz, 1H), 7.51 (td, J = 7.8, 1.2 Hz, 1H), 7.41 (t, J = 7.4 Hz, 1H), 7.06 (d, J = 15.3 Hz, 1H), 3.87 (s, 3H), 3.43 (t, J = 5.8 Hz, 4H), 2.74 (t, J = 6.2 Hz, 4H), 1.90 (p, J = 6.4 Hz, 4H), 1.70 (s, 6H). ^{13}C NMR (126 MHz, DMSO-D6) δ 178.45, 153.92, 149.76, 142.63, 129.13, 127.26, 123.06, 122.14, 113.35, 103.59, 50.76, 50.47, 33.00, 27.36, 27.02, 20.99. HRMS m/z: founded 357.2325 (calcd for $C_{26}H_{29}N_2^+$: 357.2353).

จุฬาลงกรณ์มหาวิทยาลัย
Chulalongkorn University

2.3.3 4-(diphenylamino) benzaldehyde

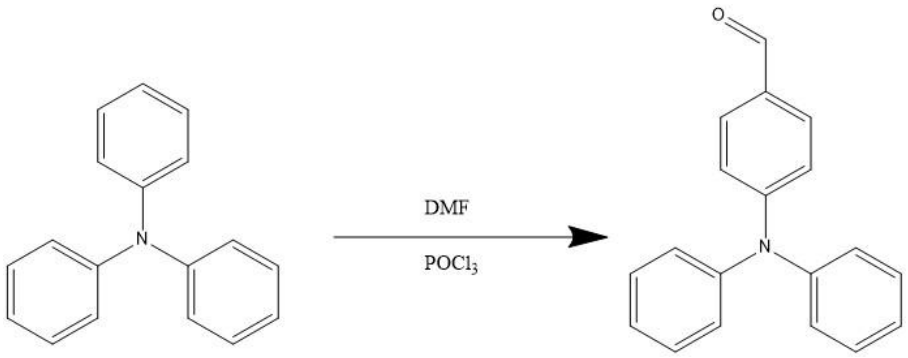

Triphenylamine (0.200 g, 0.816 mmol) was dissolved in flask of dimethylformamide (4 mL) on ice bath. Phosphorus oxychloride (0.076 mL, 0.816 mmol) was slowly dropped into the flask then stirred for 30 minutes. After that, the solution was stirred at room temperature until the color of solution become darker. The mixture was refluxed for 3 hours obtaining the dark brown solution. The mixture was workup by $NaHCO_3$ resulting yellow solid precipitated out. The crude product was purified by silica gel column chromatography using gradient hexane/ethyl acetate as an eluent to give a yield in 71%. ^1H NMR (500 MHz, $CDCl_3$) δ 9.70 (s, 1H), 7.69 (d, 2H), 7.36 - 7.16 (m, 10H), 7.10 (d, 2H).

จุฬาลงกรณ์มหาวิทยาลัย
Chulalongkorn University

2.3.4 (E)-2-(4-(diphenylamino)styryl)-1,3,3-trimethyl-3H-indol-1-ium **(INT)**

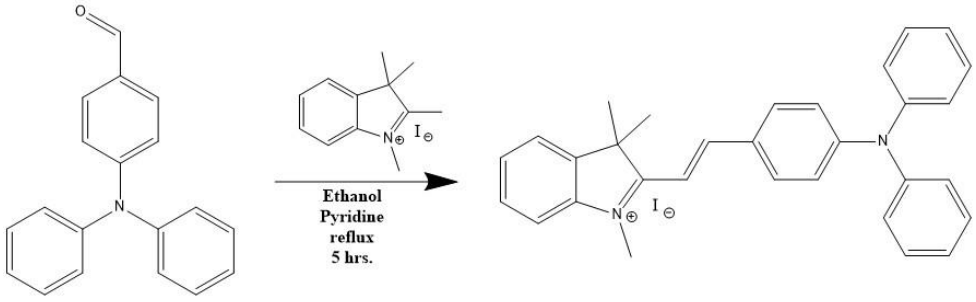

1,2,3,3-Tetramethyl-3H-indolium iodide (0.100 g, 0.332 mmol) and 4-(diphenylamino) benzaldehyde (0.091 g, 0.332 mmol) was mixed and dissolved in ethanol (5mL). Pyridine (0.04 mL, 0.498 mmol) was gently added into the flask then

refluxed for 5 hours. The reaction was cooled down and evaporated then the precipitation was performed in ethyl acetate/hexane. The crude product was purified by Sephadex G-25 column chromatography using MeOH/CH_2Cl_2 1: 2 (v/v) as an eluent. Dark pink solid was obtained in 82% yield after purification. ^{1}H NMR (500 MHz, DMSO-D6) δ 8.33 (d, J = 16.0 Hz, 1H), 8.08 – 8.02 (m, 2H), 7.86 - 7.75 (m, 2H), 7.65 - 7.50 (m, 2H), 7.48 - 7.36 (m, 6H) 7.31 - 7.19 (m, 6H), 6.91 – 6.77 (m, 2H), 4.03 (s, 3H), 1.75 (s, 6H). ^{13}C NMR (126 MHz, DMSO-D6) δ 153.50, 152.86, 145.71, 143.66, 142.46, 133.39, 130.66, 130.61, 129.39, 129.11, 127.00, 126.44, 123.31, 118.97, 115.01, 109.48, 52.08, 34.33, 26.25. DART-TOF-MS m/z: founded 429.6736 (calcd for $C_{31}H_{29}N_2^+$: 429.2325).

2.3.5 (E)-1,3,3-trimethyl-2-(2-(pyren-1-yl)vinyl)-3H-indol-1-ium (**INP**)

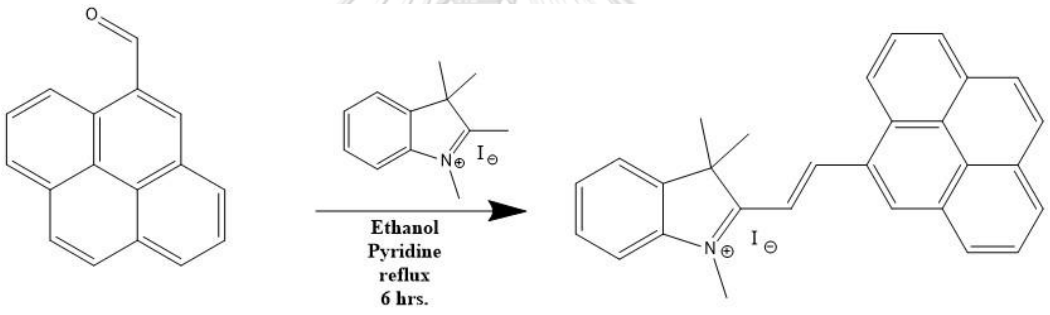

จุฬาลงกรณ์มหาวิทยาลัย
Chulalongkorn University

1,2,3,3-Tetramethyl-3H-indolium iodide (0.100 g, 0.332 mmol) and 1-pyrenecarboxaldehyde (0.076 g, 0.332 mmol) was mix and dissolve in ethanol (5mL). Pyridine (0.04 mL, 0.498 mmol) was gently added into flask then reflux for 6 hours. The reaction was to work up and recrystallized. Red solid was obtained in 91% yield after purification by column chromatography. ^{1}H NMR (500 MHz, DMSO- D6) δ 9.31 (d, J = 16.1 Hz, 1H), 9.04 (d, J = 8.4 Hz, 1H), 8.79 (d, J = 9.4 Hz, 1H), 8.56 – 8.38 (m, 5H), 8.34 (d, J = 8.9 Hz, 1H), 8.21 (t, J = 7.6 Hz, 1H), 8.05 - 7.92 (m, 3H), 7.74 - 7.63 (m, 2H) 4.29 (s, 3H), 1.96 (s, 6H). ^{13}C NMR (126 MHz, DMSO-D6) δ 182.05, 148.40, 144.06, 142.55, 134.96, 131.39, 131.31, 130.98, 130.66, 130.61, 130.05, 129.65, 128.22, 128.03, 127.91, 127.67, 126.37, 126.15, 124.54, 123.97, 123.55, 123.11, 115.88, 115.51, 52.86, 35.37, 26.26. DART-TOF-MS m/z: founded 386.9568 (calcd for $C_{29}H_{24}N^+$: 386.1903).

2.4 Studies of photophysical properties

2.4.1 Molar extinction coefficient (ε)

The molar extinction coefficient (ε) of each indolium-fluorophore conjugates were calculated from the UV absorption spectra in acetonitrile at various concentrations. The absorption intensity at maximum wavelengths of each sample was plotted against the molar concentrations. The graph had to be fit in linearity. Then, the slope of graph calculating to be the molar extinction coefficient of each indolium-fluorophore conjugates according to equation:

$$A = \varepsilon bC$$

A = the absorption intensity.

ε = molar extinction coefficient.

b = pathlength in centimeters.

C = molar concentration.

2.4.2 Relative quantum yield

Fluorescence quantum yield (ΦF) of **INJ, INT** and **INP** were carried out by using quinine sulfate in 0.1 M H_2SO_4 (ΦF = 0.54) as the standard reference. The UV-visible absorption spectra of the samples and reference were recorded under the condition that the maximum absorbance of all samples should never be above 0.1 at varied concentrations. The fluorescence emission spectra of the same samples were recorded based on the absorption maximum wavelength of each compound. The obtained data were plotted against the absorbance at the respective excitation wavelengths. The graph had to be fit in linearity with 1 interception. Additionally, the fluorescence quantum yield (ΦF) was calculated following this equation.

$$\Phi x = \Phi st \left(\frac{Gradx}{Gradst}\right)\left(\frac{\eta_x^2}{\eta_{st}^2}\right)$$

Φ_{ST} = the fluorescence quantum yield of standard reference.

Φ_X = the fluorescence quantum yield of sample.

$Grad_{ST}$ = the gradient from the plot of integrated fluorescence intensity vs absorbance of standard reference.

$Grad_X$ = the gradient from the plot of integrated fluorescence intensity vs absorbance of sample.

η_x^2 = the refractive index of standard reference.

η_{st}^2 = the refractive index of the solvent.

2.5 Studies of selectivity and sensitivity

The stock solutions of **INJ, INT** and **INP** were prepared in CH_3CN and the stock solution of metal ions were prepared in Milli-Q water. They were diluted to a desired concentration before use in further analysis.

จุฬาลงกรณ์มหาวิทยาลัย
CHULALONGKORN UNIVERSITY

2.5.1 Anions selectivity

The stock solutions of 11 anions were prepared at 10 mM in Milli-Q water by dissolving the commercial salts; NaCN, NaF, NaCl, NaBr, NaI, Na_2SO_4, Na_2SO_3, Na_2CO_3, Na_3PO_4, $NaNO_3$, $Na_2S_2O_3$.

2.5.2 Anions interference

The interference effect of other anions on the detection of CN^- was studied by adding the competing anions (10 eq higher than CN^-) into the solution of indolium fluorophore conjugates in the presence of CN^-.

2.5.3 UV-Vis and fluorescence titration and Detection limit

Various concentrations of CN^- were titrated into the solution of **INJ, INT and INP**. The final volume was adjusted to 1 mL by adding HEPES Buffer pH 8.0. UV absorbance were recorded from 0 nm to 800 nm at room temperature. On the other hands, the fluorescent intensities were recorded from 300 nm to 700 nm at room temperature using an excitation wavelength. The limit of detections (LOD) of 3 indolium fluorophore conjugates were calculated by plotting of the absorbance and fluorescence intensity of indolium fluorophore conjugates with concentrations of CN^-. The detection limit was calculated by the following equation:

$$\text{Detection limit} = \frac{3\delta}{m}$$

δ = the standard deviation of the standard deviation (S.D) of ten independent measurements of a blank.

จุฬาลงกรณ์มหาวิทยาลัย
CHULALONGKORN UNIVERSITY

m = the slope between fluorescence intensity vs. concentrations of sample.

2.6 Studies of sensing mechanism

2.6.1 Time dependent

The fluorescence intensities of **INJ, INT** and **INP** was collected after addition of CN^- in every 5 minutes for 50 minutes.

2.6.2 ^{1}H-NMR experiment

The indolium fluorophore conjugates **INT** was dissolved in DMSO-d6 and the NaCN was also dissolved in DMSO-d6. The ^{1}H-NMR spectra of **INT** with 0, 0.5 and 1 equiv of CN^- were investigated.

2.6.3 Job's plot

The concentration of three indolium fluorophore conjugates and CN^- were prepared at 10 μM. The mole fraction (X) of each indolium fluorophore conjugates were varied from 0.1 to 1.0 in this experiment. The stoichiometry of indolium fluorophore conjugates and cyanide adduct was obtained by plotting of the fluorescence intensity of indolium fluorophore conjugate's mole fraction with the mole fraction of CN^-

2.7 Application of cyanide detection

2.7.1 Cyanide quantitative analysis in real water samples

To investigated cyanide in real water samples, four water samples from four different sources; tab, pond, drinking and sea water, were studied by spiking the two difference of cyanide concentration to each water sample. The recovery in percentage was calculated from the calibration curve.

2.7.2 Cyanide detection on paper-based support

Indolium fluorophore conjugates **INJ** and **INT** were prepared in acetonitrile, then dropped 10 μL onto the paper-based support, exposed to the air until it completely dried. Various concentrations of CN^- were dropped 10 μL onto the paper-based support then observation under UV lamp.

CHAPTER III

RESULT AND DISCUSSION

3.1 Synthesis and characterization of indolium-fluorophore conjugates (INJ, INT, INP)

The synthesis of indolium fluorophore conjugates starts with N-methylation on 2,3,3-trimethyl-3H-indole to obtain the 1,2,3,3-Tetramethyl-3H-indolium iodide according to the procedure [25], the product obtained as a pink solid in a good yield (82%). In the case of 4-(diphenylamino) benzaldehyde preparation, the reaction proceeded smoothly followed by Lee and coworkers [59], the desired product was obtained in 71% after purification by silica gel column chromatography using gradient ethyl acetate/hexane as an eluent. Then, the condensation reaction between indolium moiety and aldehyde of three fluorophores; julolidine, triphenylamine, and pyrene, was performed in the presence of pyridine refluxing in ethanol for 5-6 hours providing the designed molecules; **INJ, INT** and **INP** respectively in an excellent yield (83-93%) after purification by Sephadex column chromatography (**Scheme 3.1**). The target molecules were characterized by ^{1}H-NMR, ^{13}C-NMR, and mass spectrometry.

จุฬาลงกรณ์มหาวิทยาลัย

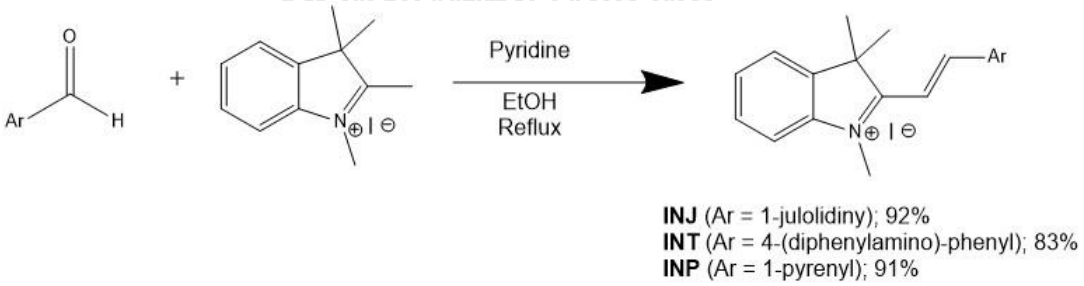

INJ (Ar = 1-julolidiny); 92%
INT (Ar = 4-(diphenylamino)-phenyl); 83%
INP (Ar = 1-pyrenyl); 91%

Scheme 3.1 Synthetic route of indolium fluorophore conjugates **INJ**, **INT** and **INP.**

For ^{1}H-NMR characterization, ^{1}H-NMR spectra of three target compounds I**NJ, INT** and **INP** which were obtained from the condensation reaction between indolium unit and corresponding aldehydes were shown in **Figure 3.1.** The peak pattern of three

compounds on the non-aromatic region was quite similar which belonging to all methyl groups on indolium unit and also non-aromatic H of julolidine on **INJ**. The characteristic peaks of H_h and H_g confirmed the presence of the π-conjugation system since they were involved in the aromatic region. The doublet peaks of H_h settled on the farthest downfield was the deshielding effect from a positive charge on indolium's nitrogen atom. ^{13}C-NMR were also collected as shown in **Figure A.4, A.8, A.11**.

Moreover, the molecular weights of **INJ, INT** and **INP** were confirmed by using a mass spectrometer (m/z = 357.23, 429.23 and 386.19 respectively) as shown in the appendix (**Figure A.5, A.9** and **A.12**)

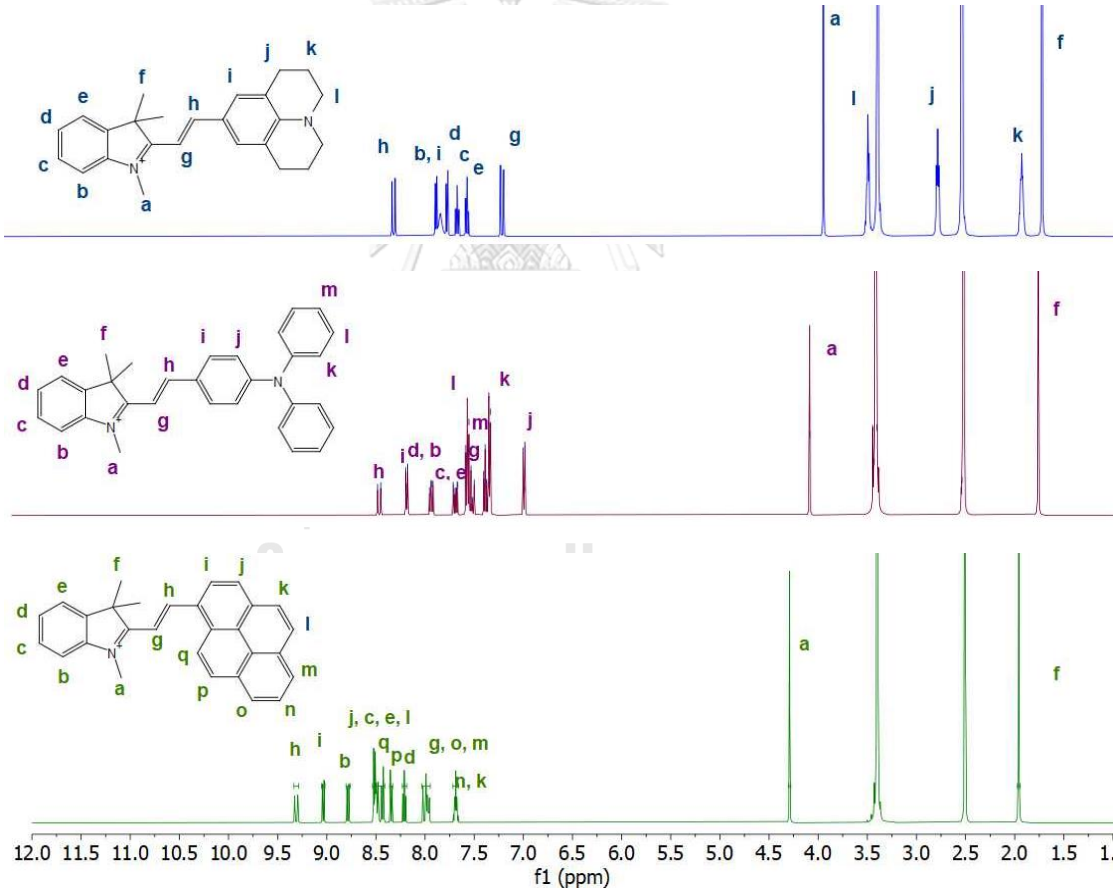

Figure 22 ^{1}H-NMR of **INJ**, **INT** and **INP** in DMSO-d6.

3.2 Photophysical properties

Absorption and emission spectra of three indolium derivatives; **INJ, INT** and **INP**, were recorded in acetonitrile showing as the bold line spectra in **Figure 3.2**. The synthesized indolium fluorophore conjugates exhibited absorption in the range of visible light resulting in three different colors of their solutions. The maximum absorption wavelengths were 594 nm, 530 nm and 495 nm for **INJ, INT** and **INP** respectively. **INP** showed the molar extinction coefficients at 20400 M^{-1} cm^{-1}. While, **INJ** and **INT** are displayed the higher of molar extinction coefficients around 55000-55400 M^{-1} cm^{-1}. In the case of fluorescence emission, fluorescence spectra of three synthesized indolium fluorophore conjugates displayed in dash line. The maximum emission wavelengths for derivatives **INJ, INT** and **INP** were observed at 612 nm, 567 and 625 nm, and 620 nm respectively. Interestingly, all of the synthesized molecules originally showed very low fluorescence intensity with the fluorescence quantum yield (ΦF) in MilliQ water obtained from a comparative method using quinine sulfate in 0.1 M H_2SO_4 (ΦF = 0.56) which were lower than 0.001.

จุฬาลงกรณ์มหาวิทยาลัย
Chulalongkorn University

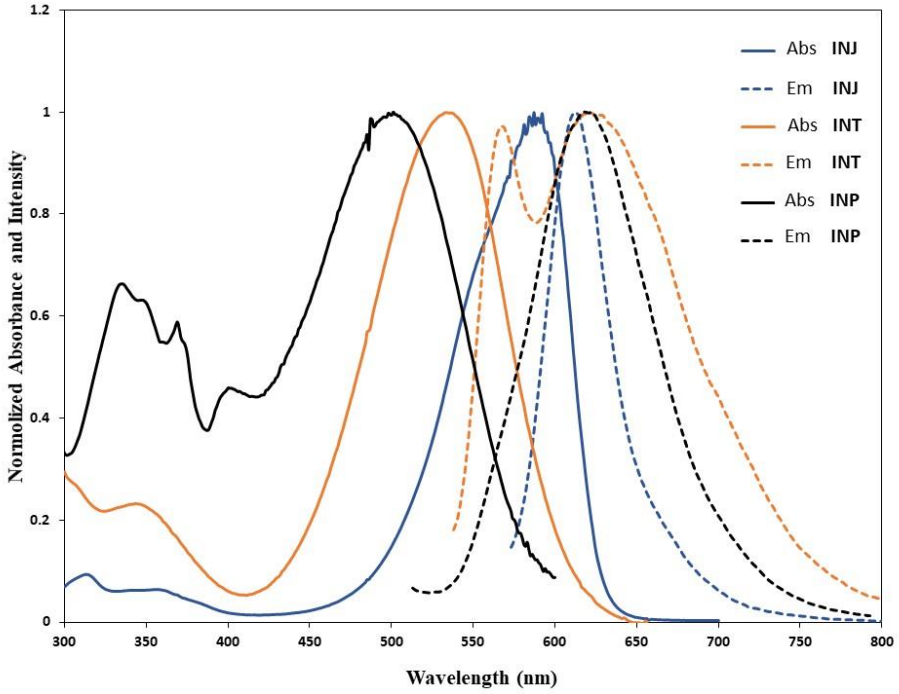

Figure 23 Normalized absorption and emission spectra of **INJ, INT** and **INP** in acetonitrile (10 μM).

Table 3.1 Photophysical properties of target molecules

Compounds	Absorption		Emission	
	λ_{max}	ε	λ_{max}	Φ
INJ	594	55000	612	<0.001
INT	530	55400	567, 625	<0.001
INP	495	20400	620	<0.001

จุฬาลงกรณ์มหาวิทยาลัย
Chulalongkorn University

3.3 Anions screening

Since the indolium moiety was expected to be a cyanide detector unit, the preliminary anions screening test of three indolium fluorophore conjugates (**INJ, INT**, and **INP**) were performed in acetonitrile. 11 anions; CN^-, SO_4^{2-}, SO_3^{2-}, F^-, Br^-, Cl^-, I^-, CO_3^{2-}, NO_3^-, PO_4^{3-} and $S_2O_3^{2-}$, were mixed with each indolium fluorophore conjugates resulting the ratiometric and fluorescence change as shown in **Figure 3.3**. There was obliviously seen that all of the synthesized compounds expressed a strong selectivity

toward cyanide ion on both colorimetric and fluorescence measurements. The colorimetric change could be observed by naked eye as a fading of solution color from violet, pink and orange into colorless. In the same way, the blueish fluorescence was discovered in all indolium fluorophore conjugates under uv light. This result was expected to be a consequence from the nucleophilic addition of CN^- onto indolium part leading to the π-conjugation interruption. Their selectivity toward anions on colorimetric and fluorescence mode will be further evaluated by spectrometer.

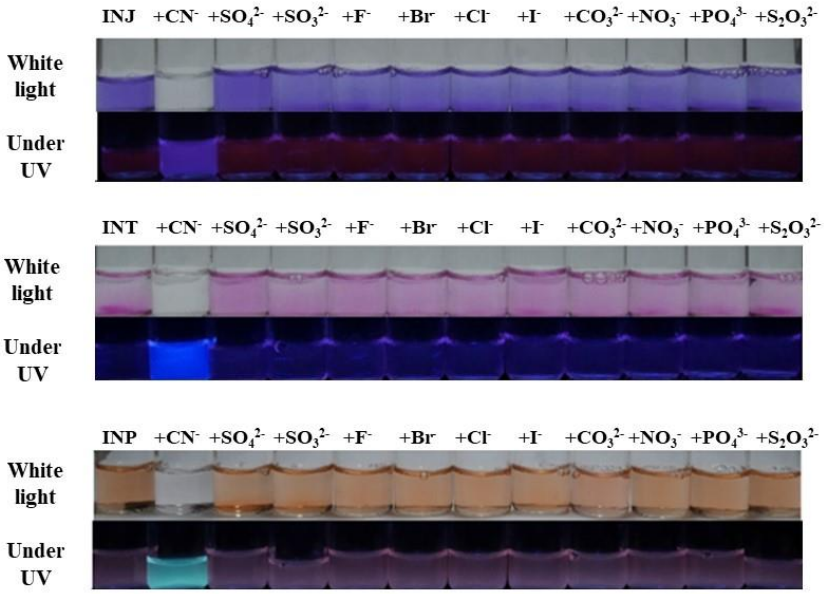

Figure 24 Fluorescence selectivity screening of **INJ**, **INT** and **INP** toward 11 types of anions in acetonitrile.

จุฬาลงกรณ์มหาวิทยาลัย
Chulalongkorn University

3.4 Optimization condition

To explore the desirable working media for synthesized indolium fluorophore conjugates, seven solvents; DMSO, DMF, THF, MeCN, EtOH, MeOH and H_2O were evaluated for preliminary of cyanide detection on **INJ**. Interestingly, most of polar organic solvents such as DMSO, DMF, THF and MeCN contributed the strong fluorescence signal while, water provided the lowest fluorescence intensity. The effect of solvent on the fluorescence signal of indolium derivatives was further studied by varying the percentage of H_2O in the acetonitrile solvent system. The result revealed

that fluorescence intensities gradually decreased upon water content in acetonitrile increased as shown in **Figure 3.4b**. There was almost no any fluorescence signal when the water was abandoned in the system more than 70%. There was a possibility that the adduct of **INJ** and CN^- via nucleophilic addition could be less soluble in water since the attacking of cyanide onto **INJ** led to the positive charge withdrawal in the indolium unit [60-62].

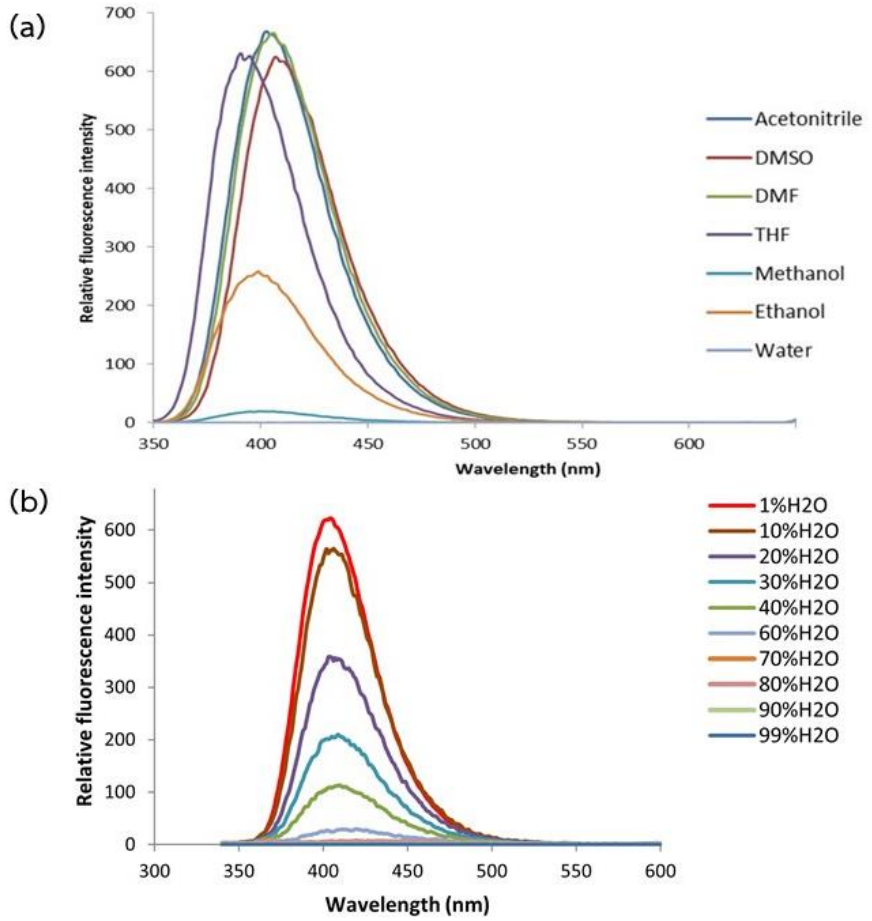

Figure 25 (a) Fluorescence spectra of **INJ** after the addition of CN^- in various solvents (b) Fluorescence spectra of **INJ** after the addition of CN^- in various percentages of H_2O in acetonitrile.

Considering that cyanide was the abandon ion which was generally found in water, the surfactant was investigated in attempt to improve the solubility of indolium

fluorophore conjugate-cyanide adduct. The evaluation of Triton-x utilizing in aqueous media on **INJ** was carried out (**Figure 3.5a).** As expectation, the presence of Triton X-100 in analysis system increased the fluorescence signals gradually, in particular, the existing of 200 μM Triton X-100 in aqueous media gave the highest fluorescence signals. This could be the result of the critical micelle concentration of Triton X-100 that settled around 0.22 mM making a good working condition. Moreover, pH also has an effect on cyanide detection of indolium fluorophore conjugates. Validation of pH indicated that there were no any fluorescence signals when the detection was performed in the strong acidic aqueous system due to, the CN^- could be protonated to HCN resulting in lack of nucleophile [63]. While, the fluorescence slightly showed up at pH 5.0 then raised significantly upon the pH increasing. To prepare indolium fluorophore conjugates sensor that could be applied in a wild range of applications, HEPES buffer pH 8.0 in the presence of 200 μM Triton X-100 was selected for further investigation.

จุฬาลงกรณ์มหาวิทยาลัย
Chulalongkorn University

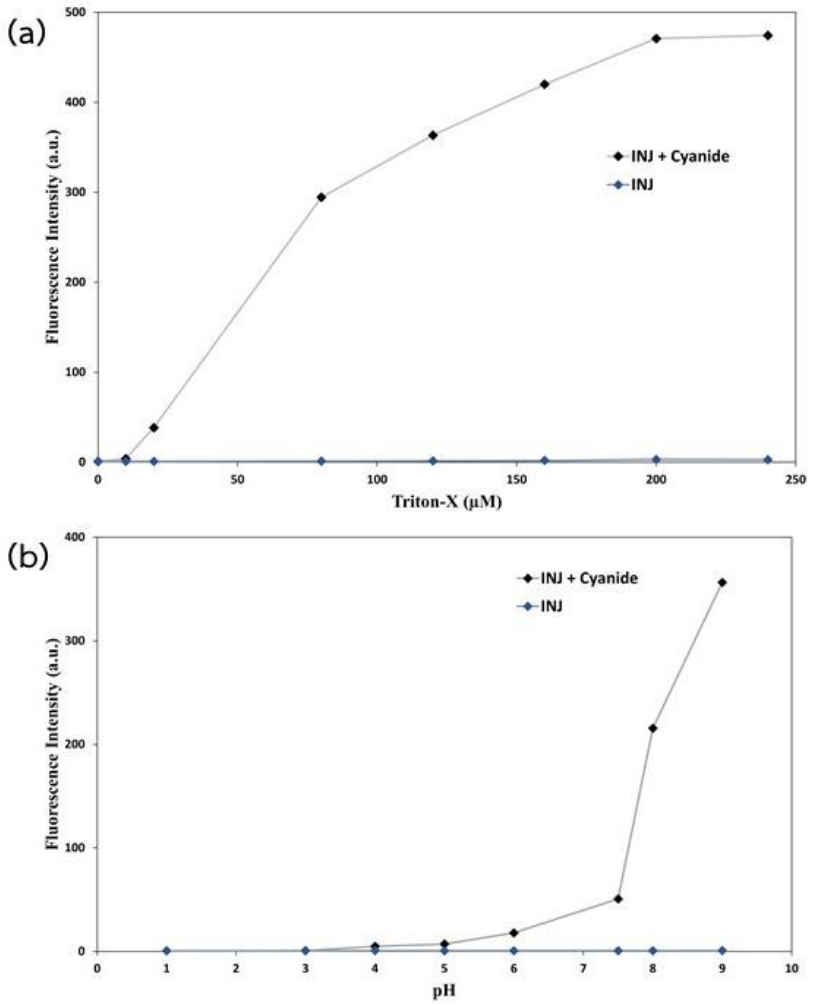

Figure 26 (a) Fluorescence intensity plot of **INJ** (10 μM) in MilliQ water in the presence of Triton X-100 at various concentration, with CN^- (10 μM) and (b) Fluorescence intensity plot of **INJ** (10 μM) in aqueous buffer solution at various pHs, with and CN^- (10 μM).

Based on the sensing mechanism which was expected to be a reaction mode between indolium fluorophore conjugates and cyanide, the effect of mixing time was validated. The fluorescence intensities were collected in every 5 minutes starting from 0 to 50 minutes (**Figure 3.6**). As a result, the reaction of **INJ** and **INP** with cyanide was saturated after 15 minutes while **INT** took the longer time to react at around 40 minutes. This could be a result of the less rigidity of triphenyl group in INT which could

settle in the unfacilitated direction to upcoming cyanide. Therefore, the further investigations will be observed after their saturated times.

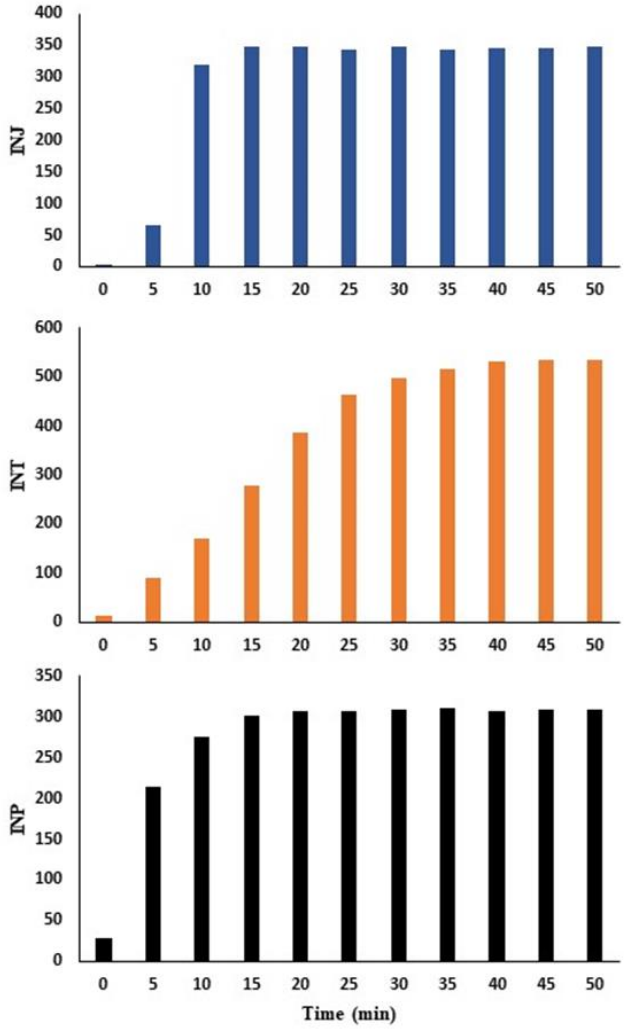

Figure 27 Sensing time observation on fluorescence intensity of **INJ, INT** and **INP** monitoring in HEPES buffer pH 8.0 in the presence of 200 μM Triton X-100 with 10 μM of CN^-

3.5 Selectivity toward cyanide

The selectivity of indolium fluorophore conjugates in colorimetric mode was accomplished by using **INJ**, **INT** and **INP** mixing with 11 different types of anions. Passionately, all of the synthesized indolium fluorophore conjugates exhibited the

strong selectivity toward CN^- over other anions in aqueous media as shown in histogram plotting by (A_0/A)-1 in **Figure 3.7**a while, other anions gave the bar chart at near zero value. Observing on absorption spectra, in the same manner to the histogram, other anions gave an almost identical of peak pattern which displayed on the range of visible light as same as the absorption peak of fluorophore itself as shown in **Figure 3.7b-d**. Whereas, CN^- was the only ion making the absorbance at 594, 530 and 495 nm in **INJ, INT** and **INP** drastically dropped down and generated the new maximum absorption on out of the range of visible region. This was the reason behind the color bleaching of their solution. As a result of nucleophilic addition of cyanide on the electrophilic carbon of indolium, the conjugation was blocked and internal charge transferred (ICT) within the molecule was inhibited.

จุฬาลงกรณ์มหาวิทยาลัย
Chulalongkorn University

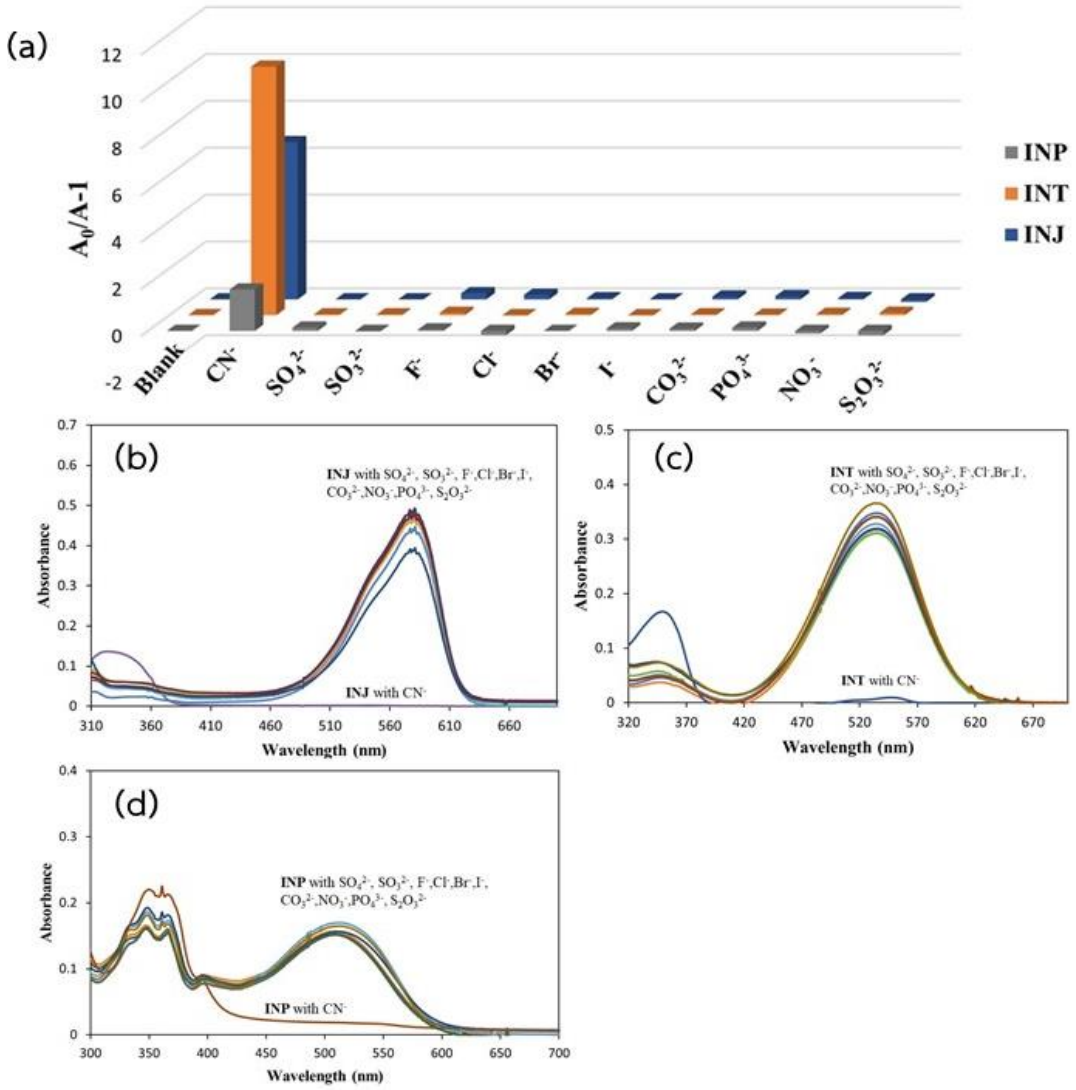

CHULALONGKORN UNIVERSITY

Figure 28 (a) Colorimetric selectivity of **INJ**, **INT** and **INP** toward 11 types of anions in HEPES buffer pH 8.0 with 200 μM Triton X-100, (b) Absorbance spectra of **INJ** with anions, (c) Absorbance spectra of **INT** with anions, (d) Absorbance spectra of **INP** with anions.

To understand more on their selectivity, the UV-Vis absorption titration of three indolium derivatives was carried out with various concentrations of CN^-. In the case of **INJ**, the absorbance spectra displayed a decreasing of signal at 495 nm while the peak around 335 nm gradually raising upon CN^- addition. The similar pattern was observed

from **INT** and **INP**. The new maximum absorption wavelengths in the range of 300 – 350 nm were selected for excitation of each fluorophore to study the emission property.

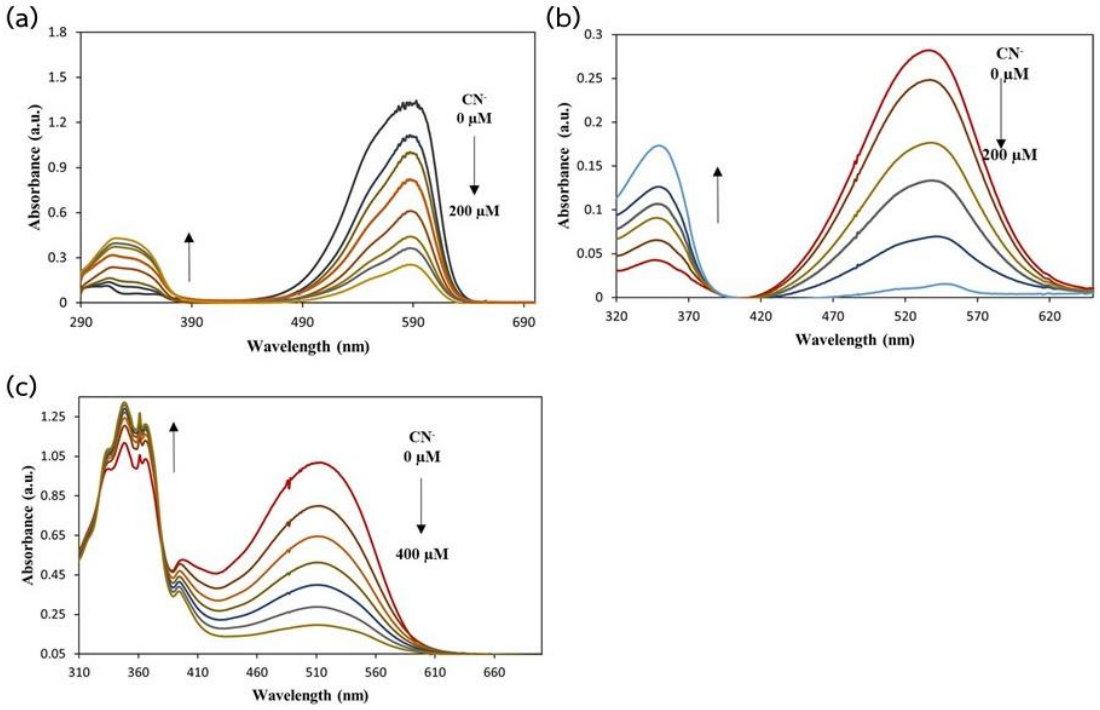

Figure 29 (a) Absorbance spectra of **INJ** upon increasing of CN^-, (b) Absorbance spectra of **INT** upon increasing of CN^-, (c) Absorbance spectra of **INP** upon increasing of CN^-.

จุฬาลงกรณ์มหาวิทยาลัย
Chulalongkorn University

The selectivity toward cyanide of indolium fluorophore conjugates on fluorescence mode was explained on the histogram in **Figure 3.9a.** Results express in a similar way with the colorimetric mode, all of synthesized derivatives showed outstanding selectivity against cyanide as a turn-on fluorescence sensor. Whereas, the addition of other anions could not induce any significant changes of the signals, cyanide could rise the fluorescence signal which is located around 400-500 nm by using excitation wavelengths at 335, 345 and 348 nm for **INJ, INT** and **INP** respectively. The fluorescence enhancement was attributed to disappearing of electron acceptor

after cyanide addition related to the ICT and PET fluorescence quenching processes [25, 64].

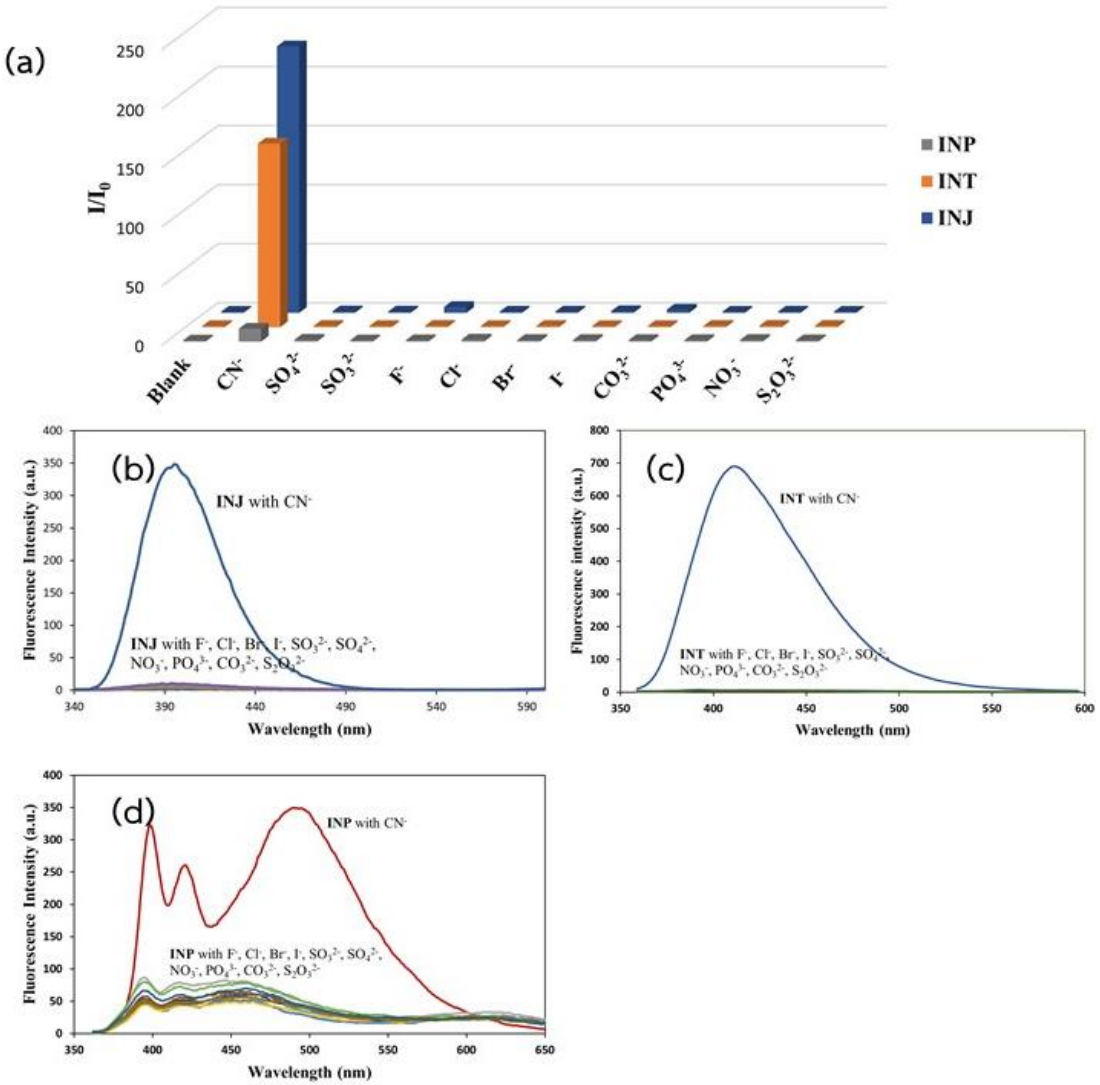

Figure 30 (a) Fluorescence selectivity of **INJ, INT** and **INP** toward 11 types of anions in HEPES buffer pH 8.0 with 200 μM Triton X-100, (b) Fluorescence spectra of INJ with anions, (c) Fluorescence spectra of **INT** with anions, (d) Fluorescence spectra of **INP** with anions.

To further demonstrate their selectivity against CN^-, these indolium derivatives were covered by anion interference test (**Figure 3.10)**. Incredibly, based on

fluorescence intensity of all synthesized compounds, there is no significant interference effect from other anions on these derivatives suggesting that synthesized indolium fluorophore conjugates could be utilized for cyanide detection in real samples without any interferent.

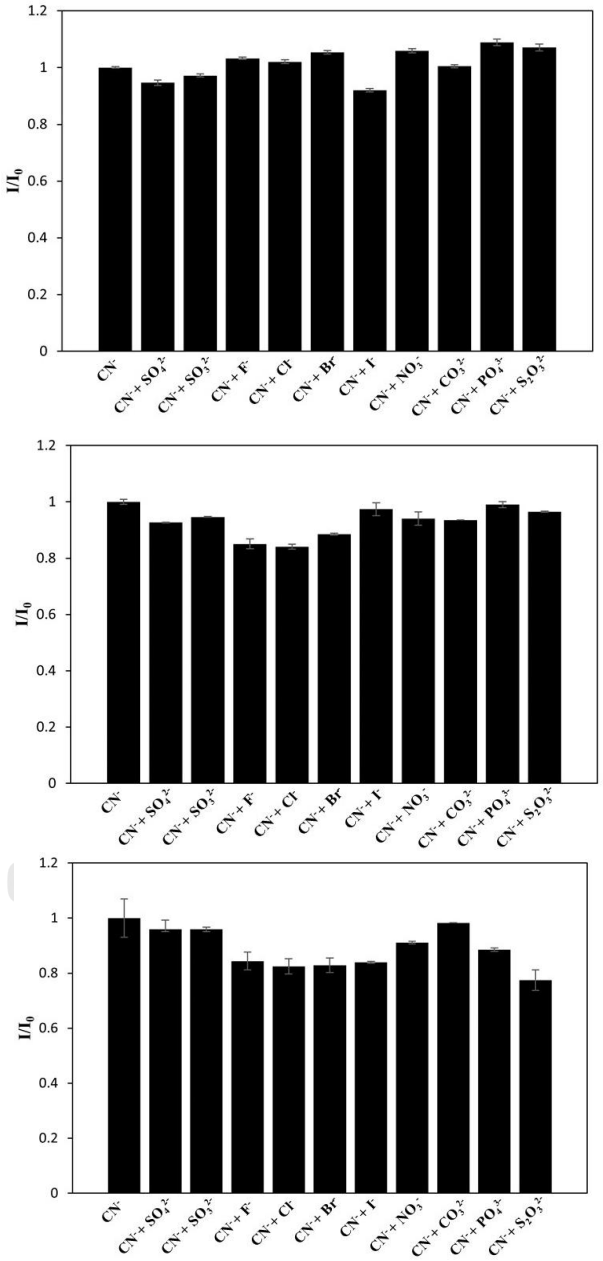

Figure 310 Interference test for **INJ, INT** and **INP** with CN^- 10 μM in the presence of other anions (100 μM) in HEPES buffer pH 8.0 with 200 μM Triton X-100

3.6 Sensitivity toward cyanide

To study their working range on colorimetric mode and the lowest concentration that the synthesized probe could detect, the UV-vis absorbance was observed upon increasing of cyanide concentration. The results revealed that the absorbance of three indolium fluorophore conjugates on the maximum wavelength around 400-500 nm decreased continuously during the addition of CN^-. The calibration curve was plotted between A_0/A and concentration of CN^- to calculate the limit of detection (LOD). In the case of **INJ**, the linearity was taken as R^2 = 0.9918 and limit of detection was calculated to be 1.87 μM which indicated a quite good sensitivity compared to the previous reports of sensor for cyanide detection. On the other hands, **INP** gave the moderate sensitivity showing with 3.65 μM of LOD. Interestingly, **INT** presented the linear relationship with the highest sensitivity and the limit of detection was found to be 0.65 μM (**Figure 3.11**). **INJ** and **INT** had a detection limit lower than the cyanide concentration that guide by WHO (1.9 μM) which supported that these compounds could be operated in the condition was guided by WHO.

จุฬาลงกรณ์มหาวิทยาลัย
Chulalongkorn University

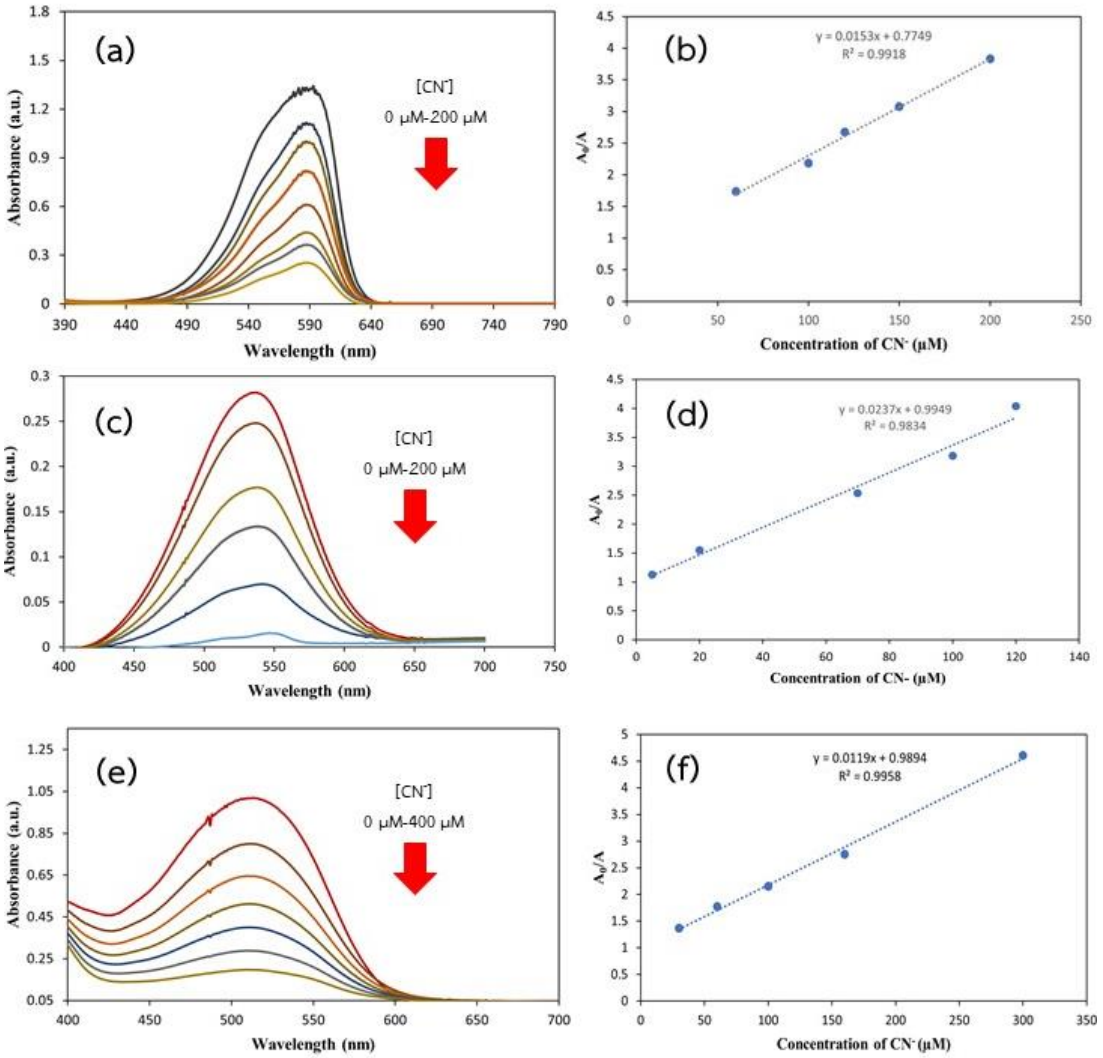

Figure 32 (a) Absorbance spectra of **INJ** during increased concentration of CN^- (b) Calibration Curve of **INJ** (c) Absorbance spectra of **INT** during increased concentration of CN^- (d) Calibration Curve of **INT** (e) Absorbance spectra of **INP** during increased concentration of CN^- (f) Calibration Curve of **INP**

The limit of detection of indolium fluorophore conjugates on fluorescence mode was also investigated, the fluorescence titration was collected upon cyanide concentration increasing. The result indicated that fluorescence intensity of **INJ**, **INT** and **INP** increased continuously when CN^- was added. The detection limit of indolium fluorophore conjugates on fluorescence mode is lower than the colorimetric which also indicated the sensitivity of method. For **INJ**, the detection limit was calculated to

be 115 nM with the R^2 = 0.9972. Interestingly, **INT** still showed the best performance toward cyanide considering by LOD at 24 nM. In similarly, **INP** displayed the lowest sensitivity with their limit of detection as 1180 nM. The calculated limit of detection from all of synthesized indolium fluorophore conjugates are lower than cyanide standard guided by FDA (1.2 μM) and WHO (1.9 μM) suggesting that all of indolium fluorophore conjugates could be operated well in samples that contained the cyanide content lower than the standard guidance. The performance of indolium fluorophore conjugates for cyanide detection was summarized in **table 3.2**

จุฬาลงกรณ์มหาวิทยาลัย
Chulalongkorn University

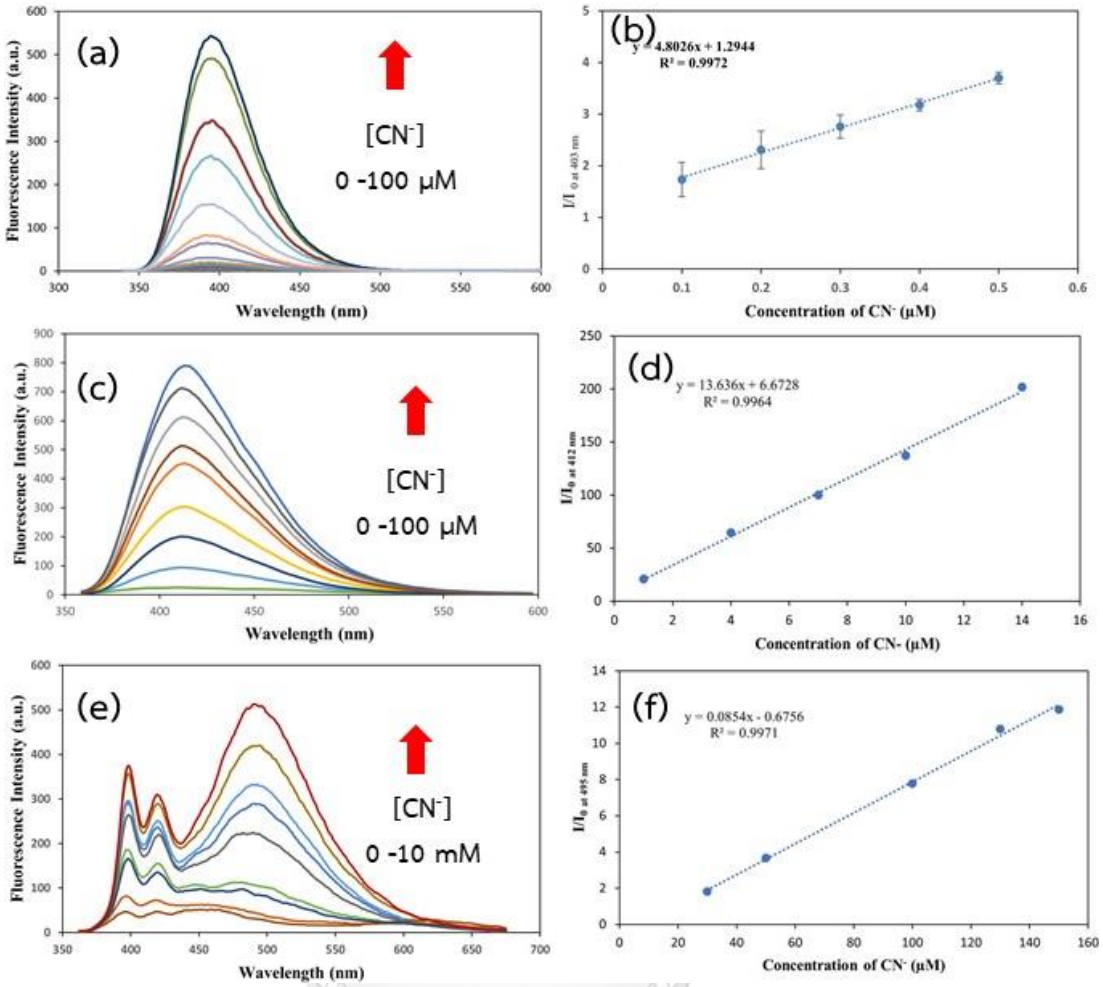

Figure 33 (a) Fluorescence spectra of **INJ** during increased concentration of CN^- (b) Calibration Curve of **INJ** (c) Fluorescence spectra of **INT** during increased concentration of CN^- (d) Calibration Curve of **INT** (e) Fluorescence spectra of **INP** during increased concentration of CN^- (f) Calibration Curve of **INP**

จุฬาลงกรณ์มหาวิทยาลัย
Chulalongkorn University

Table 3.2 Performance of indolium fluorophore conjugates as a cyanide sensor.

Compounds	Colorimetric mode		Fluorescence mode		
	λ_{abs} (nm)	LOD (μM)	λ_{ex} (nm)	λ_{em} (nm)	LOD (nM)
INJ	594	1.87	335	403	115
INT	530	0.65	345	412	24
INP	495	2.65	348	491	1180

3.7 Sensing mechanism

3.7.1 Job's plot

To evaluate the stoichiometric ratio between indolium fluorophore conjugates and cyanide, Job's plot graphs were carried out. The results showed a similar pattern of graph in all indolium fluorophore conjugates which indicated that 0.5 mole fraction of synthesized derivatives and cyanide gave the highest fluorescence intensities as shown in **Figure**. This graph pattern clarified that the stoichiometric ratio of cyanide onto each indolium fluorophore conjugate were 1:1.

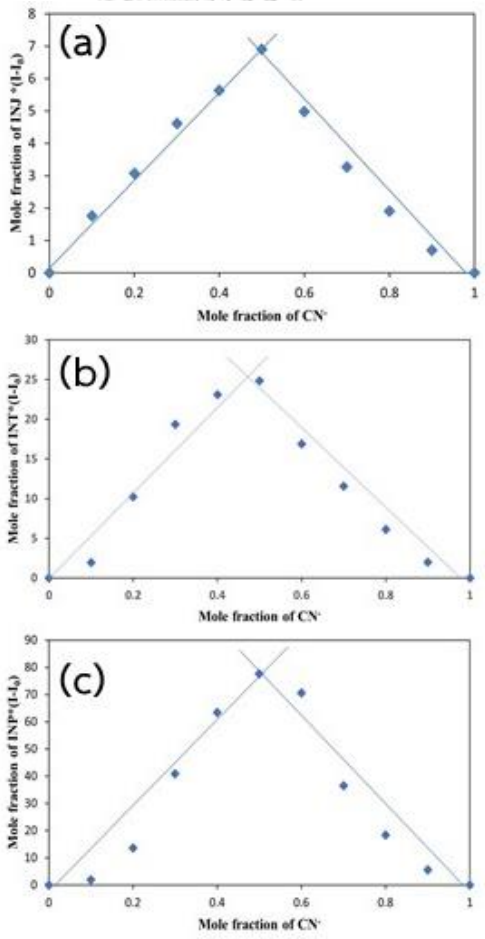

Figure 34 (a) Job's plot from fluorescence intensities of **INJ** with mole fraction CN- monitoring at 403 nm, (b) Job's plot from fluorescence intensities of **INT** mole fraction with CN^- monitoring at 412 nm and (c) Job's plot from fluorescence intensities of **INP** with CN^- monitoring at 491 nm.

3.7.2 ^{1}H-NMR experiment

To examine the structure of indolium fluorophore conjugates and cyanide adduct and confirm their reaction, **INT** was chosen for ^{1}H-NMR experiment. The observation proceeded by using DMSO-d6 as a solvent on both **INT** and cyanide at 3 ratios; 1:0, 1:0.5, and 1:1 respectively as shown in **Figure 3.14**. The significant peaks shifting was obliviously observed in non-aromatic region. Since the positive charge disappear after the addition of cyanide, signal of methyl on N atom shifted upfield from 4.0 to 2.7 ppm. Signal The two methyl groups at the 3-position of indole also shifted slightly upfield and separated into two peaks since they became two diastereotopic groups. The removal of positive charge also showed the effect on proton position H and G, peaks shifted to upfield also observed.

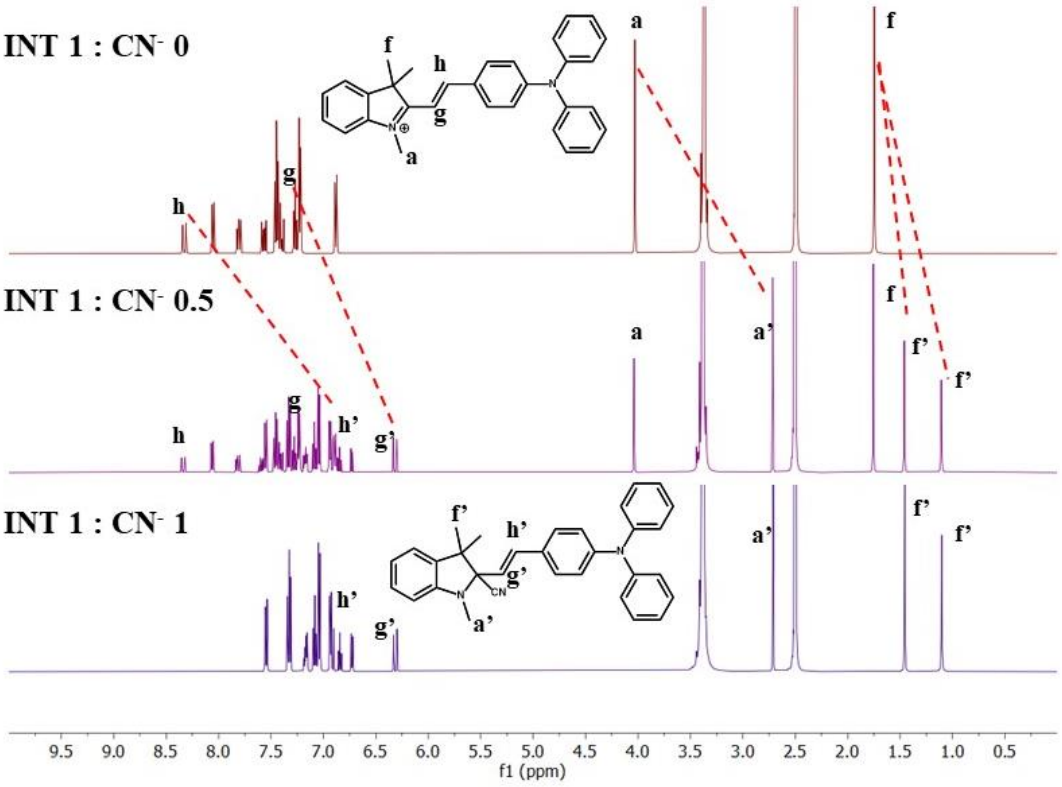

Figure 35 ^{1}H-NMR of **INT** before and after the addition of CN^{-} 0.5 and 1 equivalent monitoring in DMSO-d6.

3.7.3 Mass spectrometry experiment

Moreover, mass spectrometry was used to confirm the molecular mass of **INT**-CN adduct. The exact mass of [**INT**-CN+H^+]$^+$ was calculation as 456.23 and the data that discovered by DART-TOF MS was corresponded at 456.71 as shown in **Figure 3.15.**

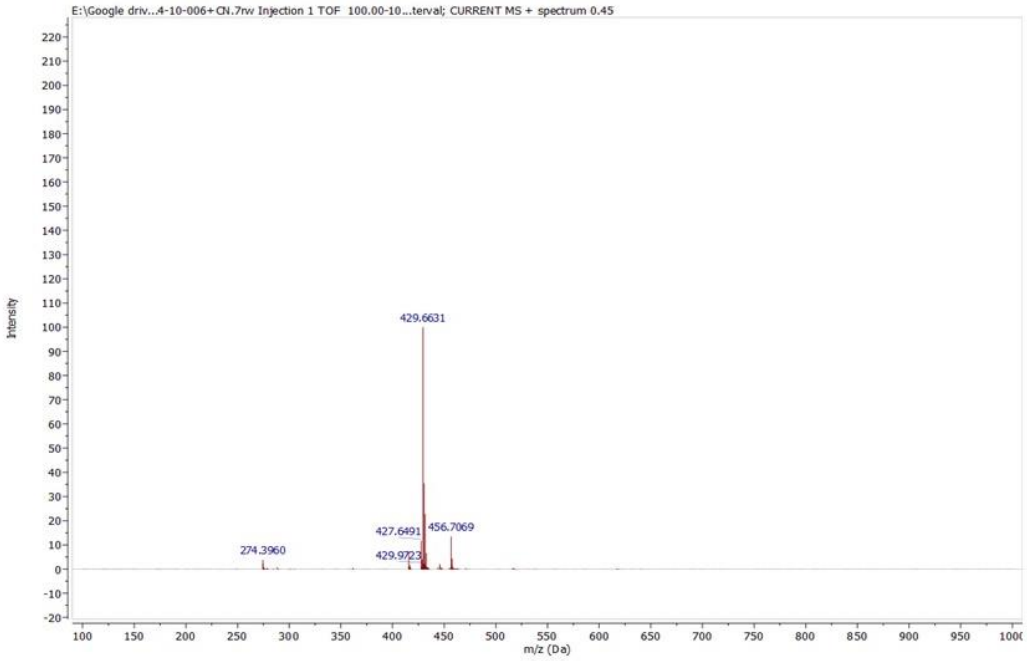

Figure 36 DART-TOF Mass spectrum of **INT**-CN adduct.

จุฬาลงกรณ์มหาวิทยาลัย
Chulalongkorn University

3.8 Utilization of indolium-fluorophore conjugates for cyanide detection

3.8.1 Quantitative analysis of cyanide in real water samples

According to sensitivity toward cyanide of synthesized indolium fluorophore conjugates, **INT** was chosen as a fluorescence sensor for quantitative analysis of cyanide in real water samples. Water from four different sources; tab, pond, drinking, and sea water were collected and spiked with two difference concentration of cyanide ion, then diluted with HEPES buffer pH 8.0. The results in **Table 3.3** indicated that **INT** could effectively detect cyanide ion in real samples with an accuracy, precision and good recovery.

Table 3.3 Quantitative analysis of CN^- in four types of water by using **INT.**

Samples	CN^- spiked (μM)	CN^- found (μM)	Recovery (%)	R.S.D. (%) n =3
Tab water	1.00	0.99	98.8	4.93
	7.00	7.01	100.23	1.62
Pond water	1.00	0.99	99.03	4.62
	7.00	7.10	101.46	0.16
Drinking water	1.00	1.02	101.55	1.60
	7.00	6.99	99.84	0.83
Sea water	1.00	1.07	106.71	1.95
	7.00	7.12	101.69	0.37

จุฬาลงกรณ์มหาวิทยาลัย
Chulalongkorn University

3.8.2 Preliminary of paper-based

The paper-based sensor was prepared by pattern wax printed onto filtered paper, then dried over the hot plate prior used. **INJ** and **INT** were chosen for this experiment. Indolium fluorophore conjugates were dropped onto paper and exposed to the air until completely dried then followed by dropping of cyanide solution. The observation under room light reveals the clearly faded of color on the paper when the cyanide concentration increased as shown in **Figure 3.16**. Observation under black light also displayed the clear fluorescence on paper. **INT** responded to CN^- slightly slower than **INJ** but presented the stronger fluorescence at lower concentration of CN^-

due to the lower in their limit of detection. These results suggest the synthesized indolium fluorophore could be applied on paper-based support.

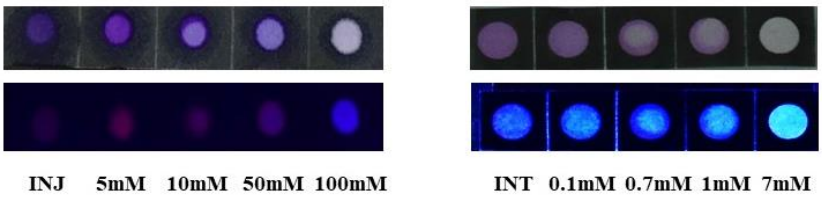

Figure 37 (a) **INJ** 10 mM on paper-based support with four different CN^- concentration (10 µL each) (b) **INT** 1 mM on paper-based support with four different CN^- concentration (10 µL each)

According to **Table 3.4**, the performance of indolium fluorophore conjugates **INJ, INT** and **INP** in comparison to others CN^- fluorescent sensors in terms of detection limit on both colorimetric and fluorescence sensing modes. **INJ** had an acceptable detection limit and ranked in the one of high sensitivity cyanide probe compared to the previous work. Remarkably, **INT** exhibited the excellent sensitivity compared to others probes with LOD in nanoscale on fluorescence and less than microscale on colorimetric mode. In comparison to Promchat's work [25], their synthesized derivative displayed the higher sensitivity with the lower in detection limit when measuring after the sonication process. The sonication could increase the solubility more than simple mixing method bringing the raise in sensitivity. However, this compound showed a slightly less sensitivity than **INT** with LOD at 49 µM when observed by using simple mixing method.

Table 3.4 Comparison sensitivity of CN^- fluorescence sensors.

Sensors	Solvent	Sensing mode	LOD (μM)	Ref.
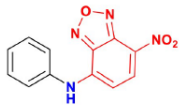	DMSO	Colorimetric	0.605	[65]
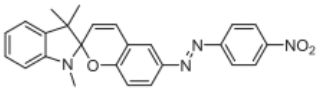	MeCN/H_2O	Colorimetric	0.65	[66]
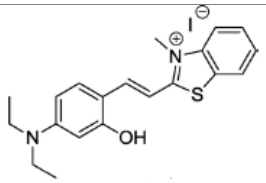	H_2O/MeOH	Colorimetric	3.6	[67]
		Fluorescence	0.5	
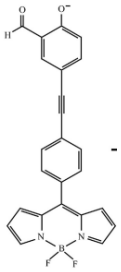	DMSO/Tris buffer pH 7.0	Fluorescence	0.88	[68]
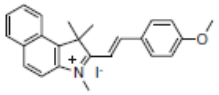	H_2O	Fluorescence	0.046	[69]
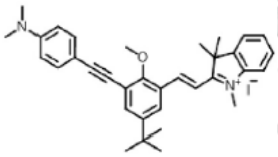	HEPES pH 6.0 with Triton X-100	Colorimetric	1.9	[25]
		Fluorescence	0.00054*	
INJ	HEPES pH 8.0 with Triton X-100	Colorimetric	1.87	This work
		Fluorescence	0.115	
INT	HEPES pH 8.0 with Triton X-100	Colorimetric	0.65	This work
		Fluorescence	0.024	
INP	HEPES pH 8.0 with Triton X-100	Colorimetric	2.65	This work
		Fluorescence	1.18	

*After sonication

จุฬาลงกรณ์มหาวิทยาลัย
Chulalongkorn University

CHAPTER IV

CONCLUSIONS

The three indolium fluorophore conjugates (**INJ, INT**, and **INP**) were successfully synthesized in good yield. As the hypothesis, all of synthesized compounds displayed the strong selectivity toward cyanide ion in aqueous solution system without any interference effect. The selectivity could be observed on be colorimetric and fluorescence measurement. Indolium conjugated with triphenylamine (**INT**) exhibit the excellent limit of detection at 24 nM on fluorescence mode and 0.65 μM on colorimetric mode which are more sensitive in comparison to the most of cyanide fluorescent probes over previous decade. Their sensing mechanism undergo nucleophilic addition onto indolium receptor unit which was confirmed by ^{1}H-NMR and ^{13}C-NMR experiment, Job's plot and mass spectrometry. Importantly, **INT** can be utilized for analysis of cyanide in real water samples with a good recovery and precision. Moreover, paper-based sensor for on-site cyanide detection was developed successfully.

จุฬาลงกรณ์มหาวิทยาลัย
Chulalongkorn University

REFERENCES

1. Lichtman, J.W. and J.-A. Conchello, *Fluorescence microscopy.* Nature Methods, 2005. **2**(12): p. 910-919.
2. Lakowicz, J.R., *Principles of Fluorescence Spectroscopy*. 3rd ed. 2006.
3. Kaur, B., N. Kaur, and S. Kumar, *Colorimetric metal ion sensors – A comprehensive review of the years 2011–2016.* Coordination Chemistry Reviews, 2018. **358**: p. 13-69.
4. Ariztia, J., et al., *PET/Fluorescence Imaging: An Overview of the Chemical Strategies to Build Dual Imaging Tools.* Bioconjugate Chemistry, 2022. **33**(1): p. 24-52.
5. de Silva, A.P., T.S. Moody, and G.D. Wright, *Fluorescent PET (Photoinduced Electron Transfer) sensors as potent analytical tools.* The Analyst, 2009. **134**(12).
6. Koide, Y., et al., *Evolution of Group 14 Rhodamines as Platforms for Near-Infrared Fluorescence Probes Utilizing Photoinduced Electron Transfer.* ACS Chemical Biology, 2011. **6**(6): p. 600-608.
7. Daly, B., J. Ling, and A.P. de Silva, *Current developments in fluorescent PET (photoinduced electron transfer) sensors and switches.* Chemical Society Reviews, 2015. **44**(13): p. 4203-4211.
8. Wu, L., et al., *Forster resonance energy transfer (FRET)-based small-molecule sensors and imaging agents.* Chem Soc Rev, 2020. **49**(15): p. 5110-5139.
9. Clegg, R.M., *Chapter 1 Förster resonance energy transfer—FRET what is it, why do it, and how it's done*, in *Fret and Flim Techniques*. 2009. p. 1-57.
10. Sekar, R.B. and A. Periasamy, *Fluorescence resonance energy transfer (FRET) microscopy imaging of live cell protein localizations.* J Cell Biol, 2003. **160**(5): p. 629-33.
11. Tasior, M., et al., *An internal charge transfer-dependent solvent effect in V-shaped azacyanines.* Org Biomol Chem, 2015. **13**(48): p. 11714-20.

จุฬาลงกรณ์มหาวิทยาลัย
Chulalongkorn University

12. Rout, Y., et al., *Tuning the Fluorescence and the Intramolecular Charge Transfer of Phenothiazine Dipolar and Quadrupolar Derivatives by Oxygen Functionalization.* J Am Chem Soc, 2021. **143**(26): p. 9933-9943.
13. Yu, F., et al., *An ICT-based strategy to a colorimetric and ratiometric fluorescence probe for hydrogen sulfide in living cells.* Chemical Communications, 2012. **48**(23).
14. Kwon, J.E. and S.Y. Park, *Advanced Organic Optoelectronic Materials: Harnessing Excited-State Intramolecular Proton Transfer (ESIPT) Process.* Advanced Materials, 2011. **23**(32): p. 3615-3642.
15. Sedgwick, A.C., et al., *Excited-state intramolecular proton-transfer (ESIPT) based fluorescence sensors and imaging agents.* Chemical Society Reviews, 2018. **47**(23): p. 8842-8880.
16. Chen, L., et al., *Excited-State Intramolecular Proton Transfer (ESIPT) for Optical Sensing in Solid State.* Advanced Optical Materials, 2021. **9**(23).
17. Niu, G., et al., *AIE luminogens as fluorescent bioprobes.* TrAC Trends in Analytical Chemistry, 2020. **123**.
18. Wurthner, F., *Aggregation-Induced Emission (AIE): A Historical Perspective.* Angew Chem Int Ed Engl, 2020. **59**(34): p. 14192-14196.
19. Ma, J., et al., *Insights into AIE materials: A focus on biomedical applications of fluorescence.* Front Chem, 2022. **10**: p. 985578.
20. Gale, P.A. and C. Caltagirone, *Fluorescent and colorimetric sensors for anionic species.* Coordination Chemistry Reviews, 2018. **354**: p. 2-27.
21. Karuppannan, S. and J.C. Chambron, *Supramolecular chemical sensors based on pyrene monomer-excimer dual luminescence.* Chem Asian J, 2011. **6**(4): p. 964-84.
22. Galievsky, V.A., et al., *Ultrafast Intramolecular Charge Transfer and Internal Conversion with Tetrafluoro-aminobenzonitriles.* ChemPhysChem, 2005. **6**(11): p. 2307-2323.

จุฬาลงกรณ์มหาวิทยาลัย
Chulalongkorn University

23. Niu, H.-T., et al., *Cyanine dye-based chromofluorescent probe for highly sensitive and selective detection of cyanide in water.* Tetrahedron Letters, 2009. **50**(48): p. 6668-6671.

24. Park, J.H., et al., *Spontaneous optical response towards cyanide ion in water by a reactive binding site probe.* Spectrochim Acta A Mol Biomol Spectrosc, 2020. **233**: p. 118190.

25. Promchat, A., P. Rashatasakhon, and M. Sukwattanasinitt, *A novel indolium salt as a highly sensitive and selective fluorescent sensor for cyanide detection in water.* J Hazard Mater, 2017. **329**: p. 255-261.

26. Niamnont, N., et al., *A novel phenylacetylene-indolium fluorophore for detection of cyanide by the naked eye.* RSC Advances, 2015. **5**(79): p. 64763-64768.

27. Yang, Y., et al., *A new highly selective and turn-on fluorescence probe for detection of cyanide.* Sensors and Actuators B: Chemical, 2014. **193**: p. 220-224.

28. Shiraishi, Y., et al., *Rapid, selective, and sensitive fluorometric detection of cyanide anions in aqueous media by cyanine dyes with indolium-coumarin linkages.* Chem Commun (Camb), 2014. **50**(78): p. 11583-6.

29. Sun, Y., et al., *Ratiometric fluorescent probe for rapid detection of bisulfite through 1,4-addition reaction in aqueous solution.* J Agric Food Chem, 2014. **62**(15): p. 3405-9.

30. Liu, S., et al., *A novel "turn-on" fluorescent probe based on triphenylimidazole-hemicyanine dyad for colorimetric detection of CN(-) in 100% aqueous solution.* J Hazard Mater, 2018. **344**: p. 875-882.

31. Li, J., et al., *A novel colorimetric and fluorescent probe based on indolium salt for detection of cyanide in 100% aqueous solution.* Dyes and Pigments, 2019. **168**: p. 175-179.

32. Cheng, S., et al., *A coumarin-connected carboxylic indolinium sensor for cyanide detection in absolute aqueous medium and its application in biological cell imaging.* Spectrochim Acta A Mol Biomol Spectrosc, 2020. **228**: p. 117710.

จุฬาลงกรณ์มหาวิทยาลัย
Chulalongkorn University

33. Morikawa, Y., et al., *A novel turn-on fluorescent sensor for cyanide ions based on the charge transfer transition of phenothiazine/indolium compounds.* Materials Advances, 2021. **2**(18): p. 6104-6111.

34. Varejão, J.O.S., E.V.V. Varejão, and S.A. Fernandes, *Synthesis and Derivatization of Julolidine: A Powerful Heterocyclic Structure.* European Journal of Organic Chemistry, 2019. **2019**(27): p. 4273-4310.

35. Ji, Y., F. Dai, and B. Zhou, *Developing a julolidine-fluorescein-based hybrid as a highly sensitive fluorescent probe for sensing and bioimaging cysteine in living cells.* Talanta, 2019. **197**: p. 631-637.

36. Sirbu, D., et al., *An unprecedented oxidised julolidine-BODIPY conjugate and its application in real-time ratiometric fluorescence sensing of sulfite.* Org Biomol Chem, 2019. **17**(31): p. 7360-7368.

37. Gutkowski, K.I., M.L. Japas, and P.F. Aramendía, *Fluorescence of dicyanovinyl julolidine in a room-temperature ionic liquid.* Chemical Physics Letters, 2006. **426**(4-6): p. 329-333.

38. Jeong, H.Y., S.Y. Lee, and C. Kim, *Furan and Julolidine-Based "Turn-on" Fluorescence Chemosensor for Detection of F(-) in a Near-Perfect Aqueous Solution.* J Fluoresc, 2017. **27**(4): p. 1457-1466.

39. Maity, D., et al., *Visible-near-infrared and fluorescent copper sensors based on julolidine conjugates: selective detection and fluorescence imaging in living cells.* Chemistry, 2011. **17**(40): p. 11152-61.

40. Choi, Y.W., et al., *A fluorescent chemosensor for Al3+ based on julolidine and tryptophan moieties.* Tetrahedron, 2016. **72**(16): p. 1998-2005.

41. Liu, F.-T., et al., *A ratiometric lysosome-targeted fluorescent probe for imaging SO2 based on the coumarin-quinoline-julolidine molecular system.* Dyes and Pigments, 2023. **210**.

42. Kim, S.Y., et al., *Intriguing emission properties of triphenylamine-carborane systems.* Phys Chem Chem Phys, 2015. **17**(24): p. 15679-82.

43. Hariharan, P.S., et al., *Molecular Engineering of Triphenylamine Based Aggregation Enhanced Emissive Fluorophore: Structure-Dependent*

จุฬาลงกรณ์มหาวิทยาลัย
Chulalongkorn University

Mechanochromism and Self-Reversible Fluorescence Switching. Crystal Growth & Design, 2016. **17**(1): p. 146-155.

44. Yang, Y., et al., *Triphenylamine, Carbazole or Tetraphenylethylene-Functionalized Benzothiadiazole Derivatives: Aggregation-Induced Emission (AIE), Solvatochromic and Different Mechanoresponsive Fluorescence Characteristics.* Molecules, 2022. **27**(15).
45. Yang, Y., B. Li, and L. Zhang, *Design and synthesis of triphenylamine-malonitrile derivatives as solvatochromic fluorescent dyes.* Sensors and Actuators B: Chemical, 2013. **183**: p. 46-51.
46. Yang, M., et al., *Aggregation-induced fluorescence behavior of triphenylamine-based Schiff bases: the combined effect of multiple forces.* J Org Chem, 2013. **78**(20): p. 10344-59.
47. Liu, Y., et al., *A series of triphenylamine-based two-photon absorbing materials with AIE property for biological imaging.* J Mater Chem B, 2014. **2**(33): p. 5430-5440.
48. Kolcu, F., D. Erdener, and İ. Kaya, *A Schiff base based on triphenylamine and thiophene moieties as a fluorescent sensor for Cr (III) ions: Synthesis, characterization and fluorescent applications.* Inorganica Chimica Acta, 2020. **509**.
49. Mohanasundaram, D., et al., *A simple triphenylamine based turn-off fluorescent sensor for copper (II) ion detection in semi-aqueous solutions.* Journal of Photochemistry and Photobiology A: Chemistry, 2022. **427**.
50. Li, D., et al., *A novel dual-response triphenylamine-based fluorescence sensor for special detection of hydrazine in water.* Materials Science and Engineering: B, 2022. **276**.
51. Ayyavoo, K. and P. Velusamy, *Pyrene based materials as fluorescent probes in chemical and biological fields.* New Journal of Chemistry, 2021. **45**(25): p. 10997-11017.
52. Goswami, S., et al., *A new pyrene based highly sensitive fluorescence probe for copper(II) and fluoride with living cell application.* Org Biomol Chem, 2014. **12**(19): p. 3037-44.

จุฬาลงกรณ์มหาวิทยาลัย
Chulalongkorn University

53. Zhao, M., et al., *Pyrene excimer-based fluorescent sensor for detection and removal of Fe(3+) and Pb(2+) from aqueous solutions.* Spectrochim Acta A Mol Biomol Spectrosc, 2017. **173**: p. 235-240.

54. Lee, M., et al., *A new bis-pyrene derivative as a selective colorimetric and fluorescent chemosensor for cyanide and fluoride and anion-activated CO2 sensing.* Sensors and Actuators B: Chemical, 2014. **199**: p. 369-376.

55. Farhangi, S. and J. Duhamel, *Probing Side Chain Dynamics of Branched Macromolecules by Pyrene Excimer Fluorescence.* Macromolecules, 2015. **49**(1): p. 353-361.

56. Zang, L., et al., *A highly specific pyrene-based fluorescent probe for hypochlorite and its application in cell imaging.* Sensors and Actuators B: Chemical, 2015. **211**: p. 164-169.

57. Tang, Y., et al., *Synthesis of a new pyrene-devived fluorescent probe for the detection of Zn2+.* Tetrahedron Letters, 2018. **59**(44): p. 3916-3922.

58. Liu, Y., et al., *A novel pyrene-based fluorescent probe for Al(3+) detection.* Spectrochim Acta A Mol Biomol Spectrosc, 2023. **287**(Pt 2): p. 122085.

59. Hye Jeong Lee, J.S., Jaehoon Hwang, and Soo Young Park, *Triphenylamine-Cored Bifunctional Organic Molecules for Two-Photon Absorption and Photorefraction.* Chem. Mater., 2004. **16**(3): p. 456-465.

60. Wang, L., et al., *Novel asymmetric Cy5 dyes: Synthesis, photostabilities and high sensitivity in protein fluorescence labeling.* Journal of Photochemistry and Photobiology A: Chemistry, 2010. **210**(2-3): p. 168-172.

61. Mertsch, A., et al., *Synthesis and application of water-soluble, photoswitchable cyanine dyes for bioorthogonal labeling of cell-surface carbohydrates.* Z Naturforsch C J Biosci, 2016. **71**(9-10): p. 347-354.

62. Park, J.W., et al., *Novel cyanine dyes with vinylsulfone group for labeling biomolecules.* Bioconjug Chem, 2012. **23**(3): p. 350-62.

63. Schulz, A. and J. Surkau, *Main group cyanides: from hydrogen cyanide to cyanido-complexes.* Reviews in Inorganic Chemistry, 2023. **43**(1): p. 49-188.

จุฬาลงกรณ์มหาวิทยาลัย
Chulalongkorn University

64. Wen, D., X. Deng, and Y. Yu, *A novel indolium salt as a rapid colorimetric probe for cyanide detection in aqueous solution.* Chemical Papers, 2020. **75**(3): p. 1095-1102.

65. Balagurusamy, B., P. Ilayaperumal, and R. Chellaiah, *Photometric and Colorimetric Cyanide Detection Sensor Using Amine Based Nitrobenzoxadiazole Derivatives.* ChemistrySelect, 2022. **7**(30).

66. Prakash, K., P. Ranjan Sahoo, and S. Kumar, *A substituted spiropyran for highly sensitive and selective colorimetric detection of cyanide ions.* Sensors and Actuators B: Chemical, 2016. **237**: p. 856-864.

67. Rao, P.G., B. Saritha, and T.S. Rao, *Highly selective reaction based colorimetric and fluorometric chemosensors for cyanide detection via ICT off in aqueous solution.* Journal of Photochemistry and Photobiology A: Chemistry, 2019. **372**: p. 177-185.

68. Sukato, R., et al., *New turn-on fluorescent and colorimetric probe for cyanide detection based on BODIPY-salicylaldehyde and its application in cell imaging.* J Hazard Mater, 2016. **314**: p. 277-285.

69. Sun, Y., et al., *A fluorescent turn-on probe based on benzo [e] indolium for cyanide ion in water with high selectivity.* J Fluoresc, 2013. **23**(6): p. 1255-61.

จุฬาลงกรณ์มหาวิทยาลัย
CHULALONGKORN UNIVERSITY

จุฬาลงกรณ์มหาวิทยาลัย
Chulalongkorn University

APPENDIX

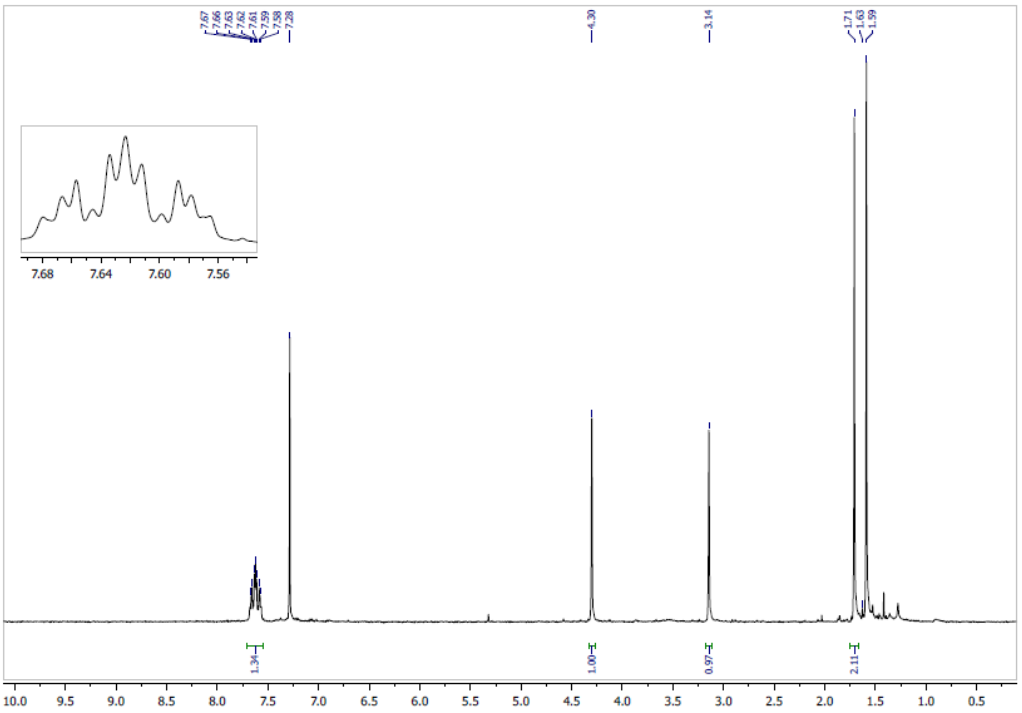

Figure 38 ^{1}H-NMR spectrum of 1,2,3,3-Tetramethyl-3H-indolium iodide in $CDCl_3$

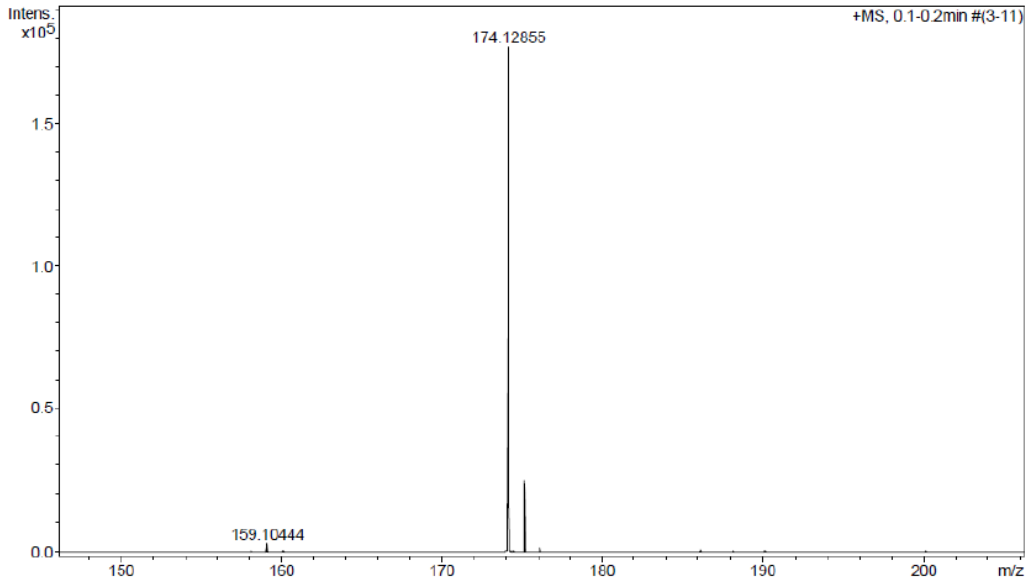

Figure 39 HRMS spectrum of 1,2,3,3-Tetramethyl-3H-indolium iodide

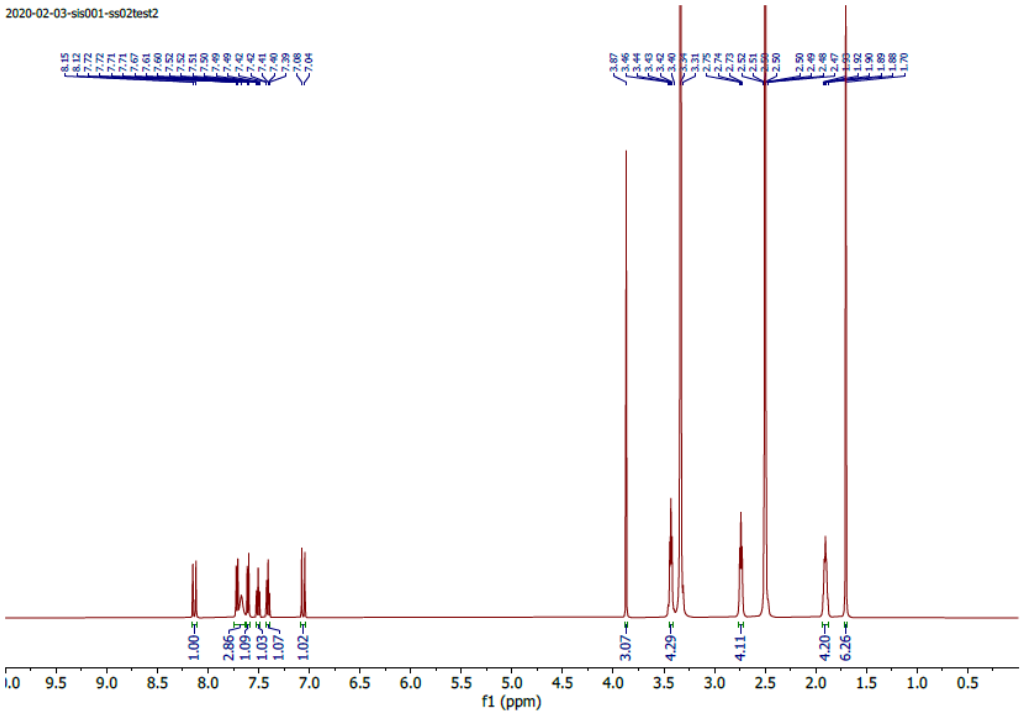

Figure 40 ^{1}H-NMR spectrum of **INJ** in DMSO-d6

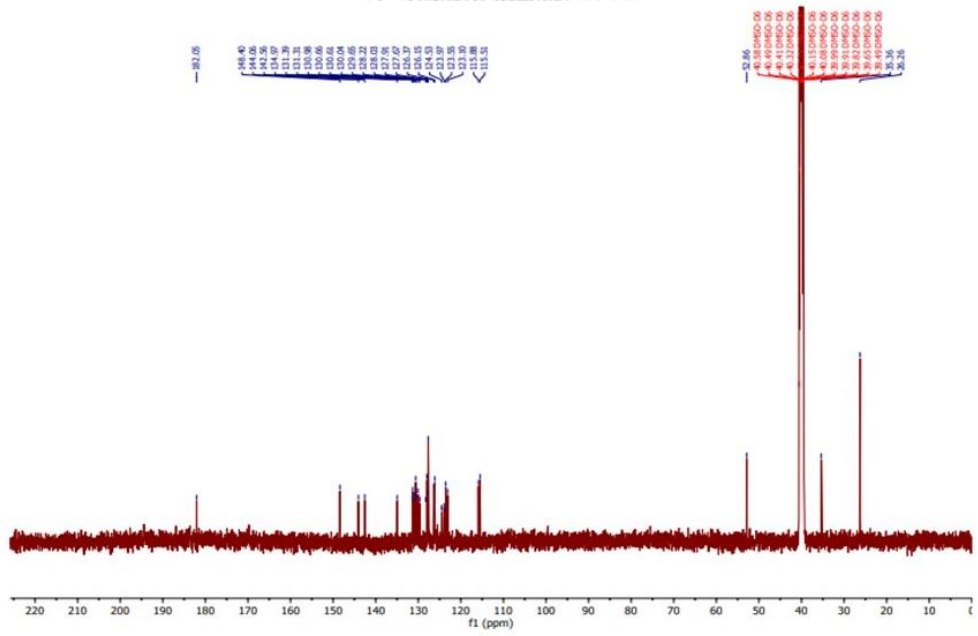

Figure 41 ^{13}C-NMR spectrum of **INJ** in DMSO-d6

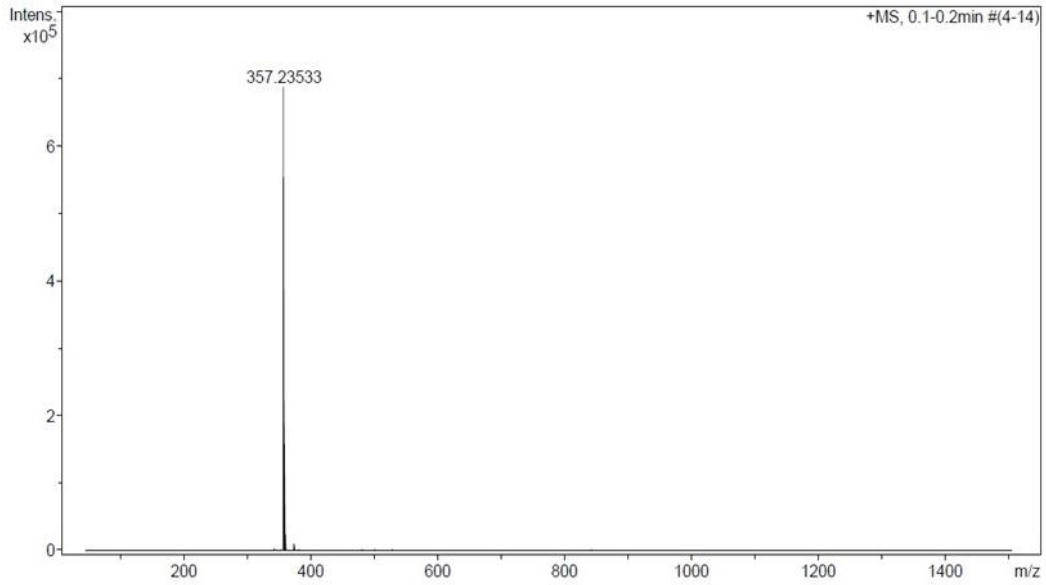

Figure 42 HRMS spectrum of **INJ**

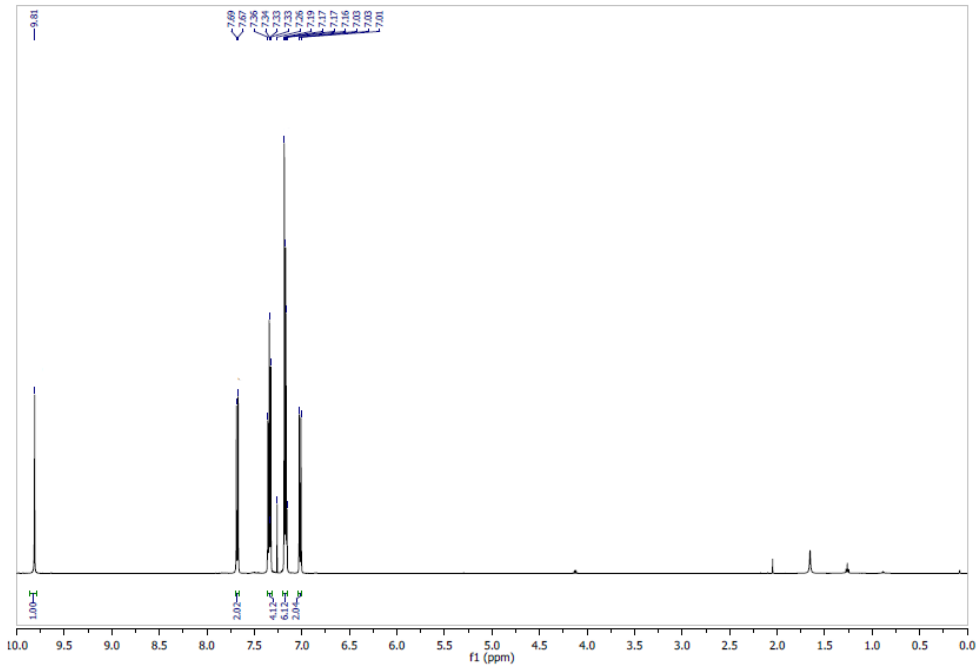

Figure 43 ^{1}H-NMR spectrum of 4-(diphenylamino) benzaldehyde in $CDCl_3$

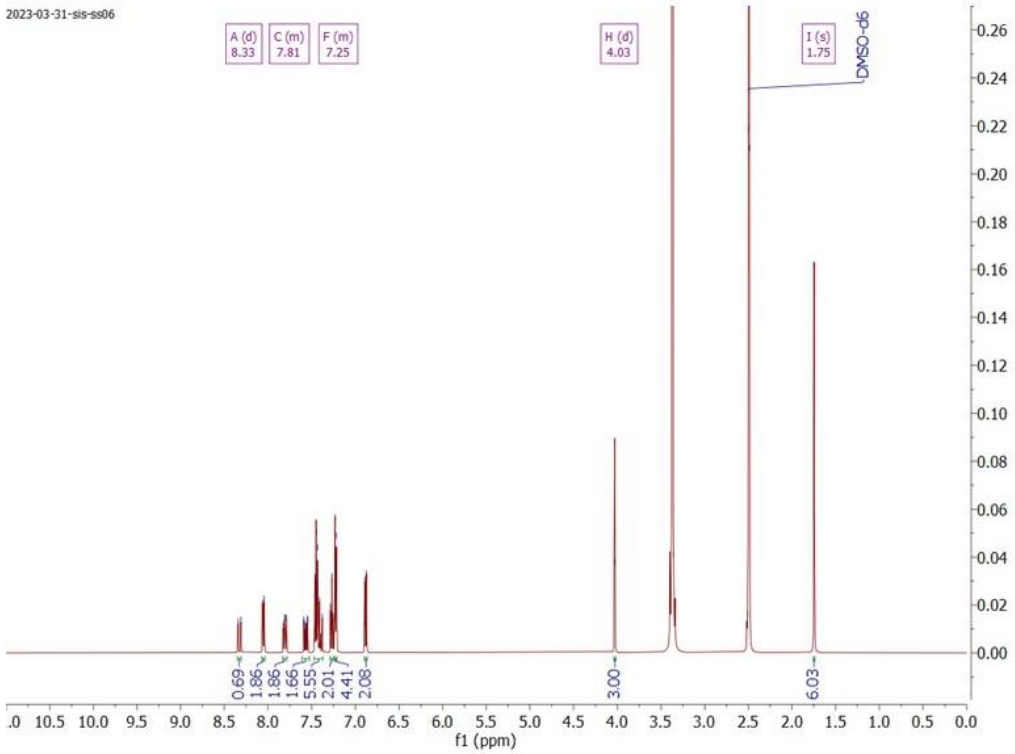

Figure 44 ^{1}H-NMR spectrum of **INT** in DMSO-d6

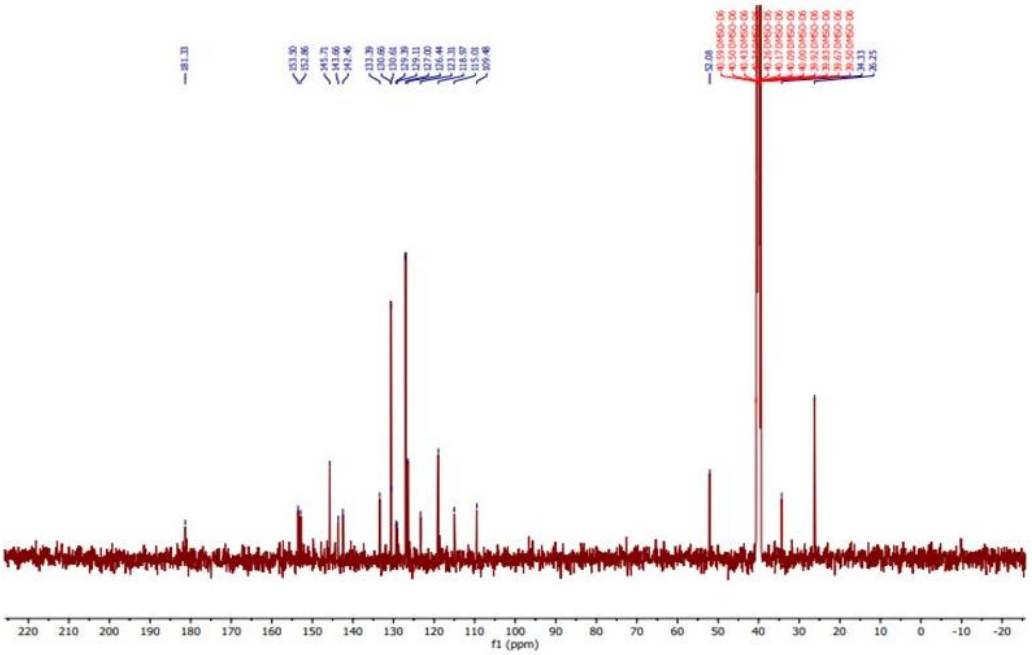

Figure 45 ^{13}C-NMR spectrum of **INT** in DMSO-d6

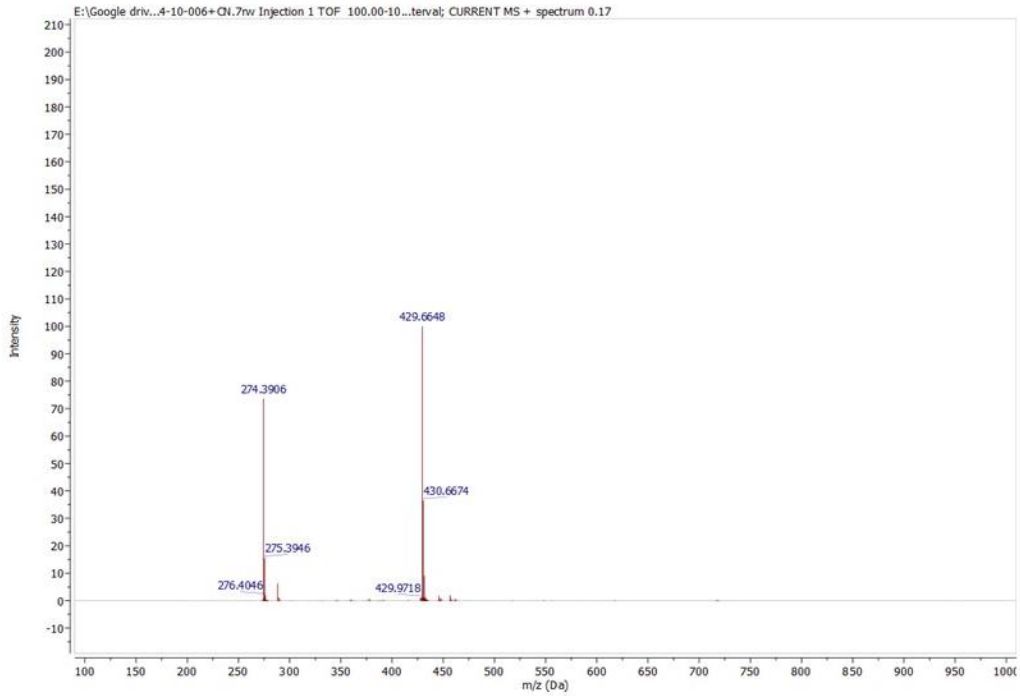

Figure 46 DART-TOF MS spectrum of **INT**

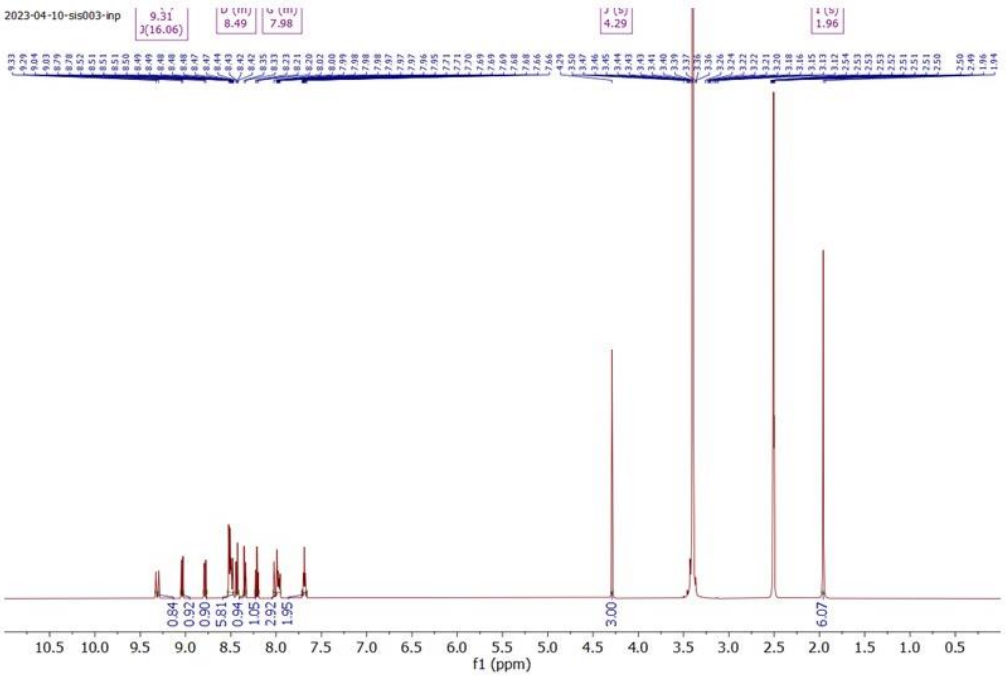

Figure 47 ^{1}H-NMR spectrum of **INP** in DMSO-d6

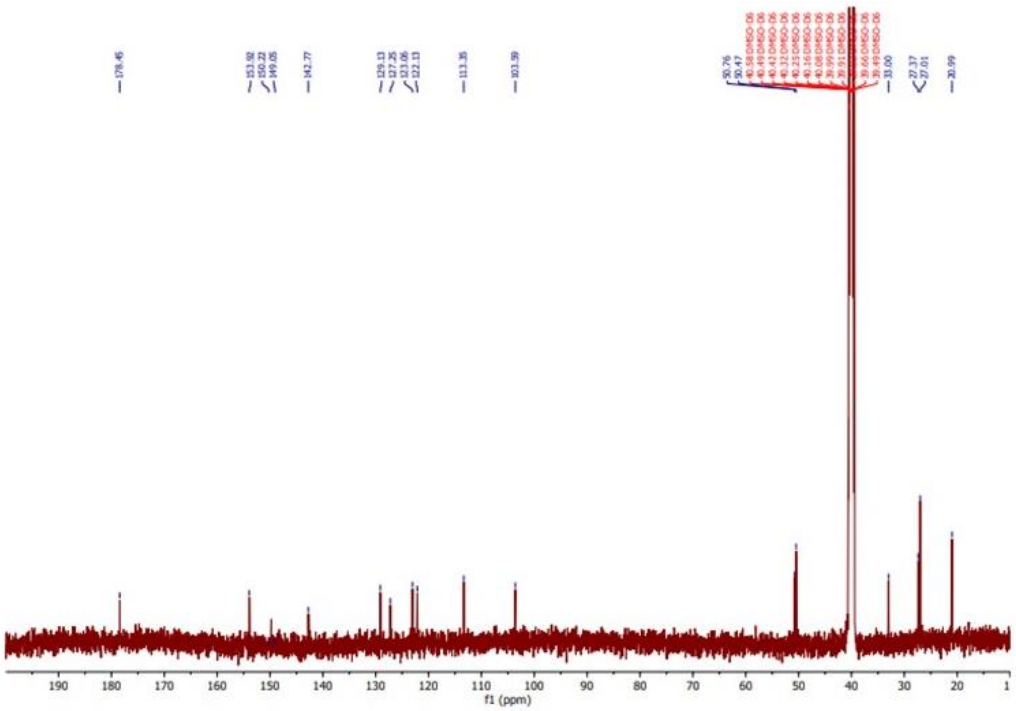

Figure 48 ^{13}C-NMR spectrum of **INP** in DMSO-d6

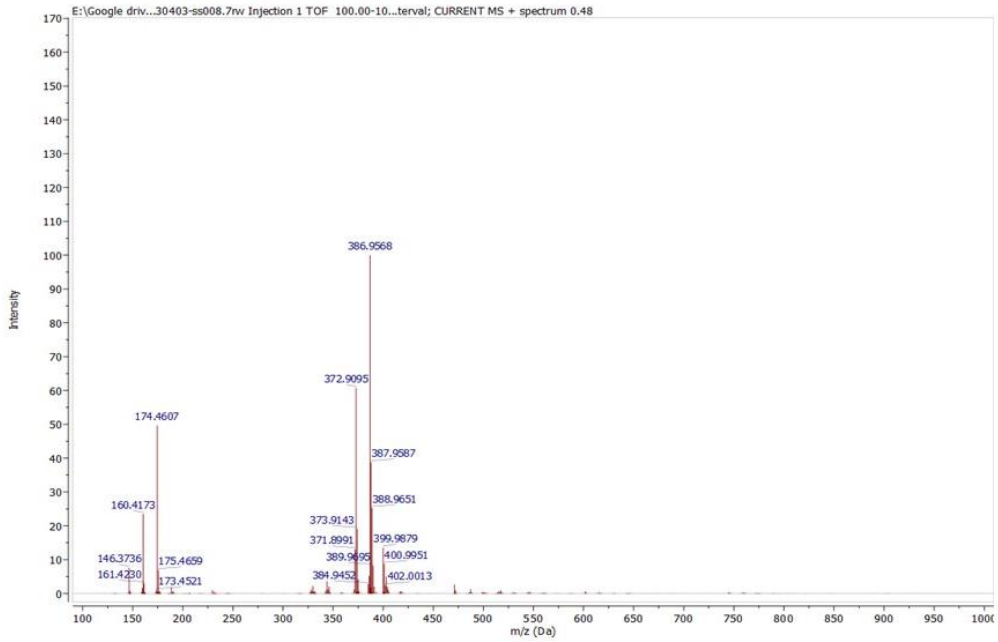

Figure 49 DART-TOF MS spectrum of **INP**

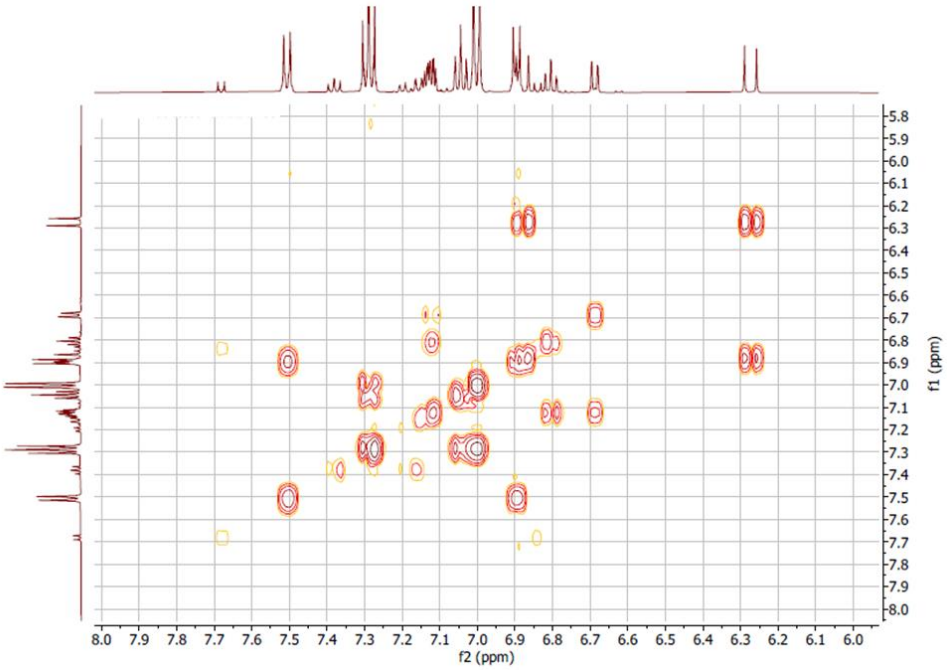

Figure 50 ^{1}H-^{1}H COSY NMR spectrum of **INT** 1: CN 0.5 in DMSO-d6

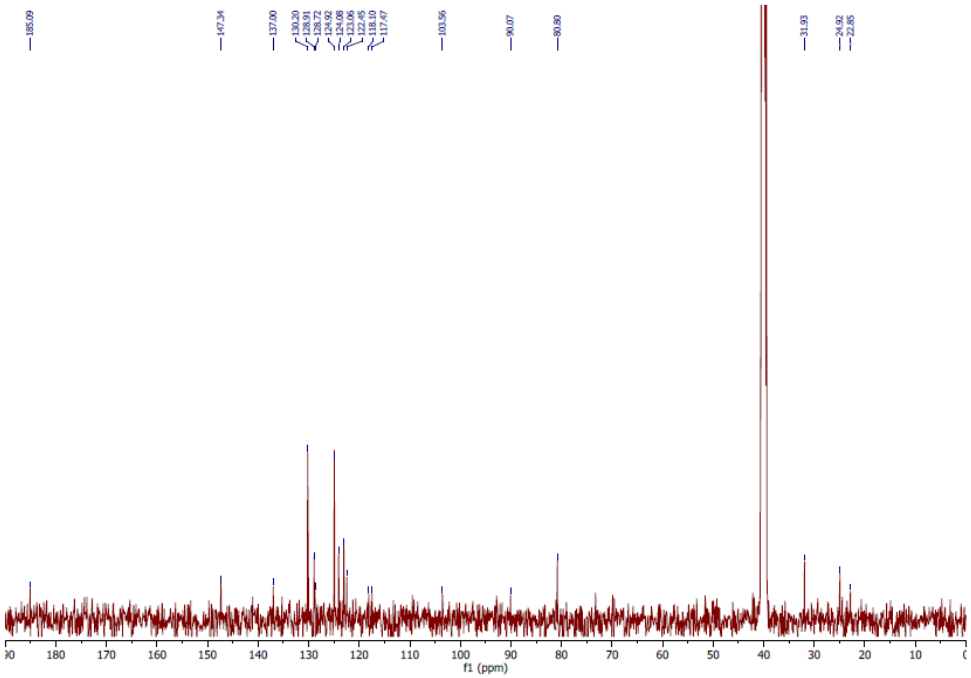

Figure 51 ^{13}C-NMR spectrum of **INT-**CN adduct in DMSO-d6

VITA

NAME	Siraporn Soonthonhut
DATE OF BIRTH	11 October 1991
PLACE OF BIRTH	Bangkok
INSTITUTIONS ATTENDED	Bachelor's Degree of Science, majoring in Chemistry, Faculty of Science and Technology, Thammasat University in 2013. Master Degree of Science, majoring in Chemistry (organic chemistry), Faculty of Science and Technology, Thammasart Universsity in 2016. Since 2017, She has been a graduate student in chemistry and become a member of Material Advancement and Proficient Synthesis (MAPS) group under supervision of Professor Dr. Paitoon Rashatasakhon. She graduated with a Ph.D. Degree in Chemistry in academic year 2022. She received the scholarship from Science Acheivement Scholarship of Thailand (SAST).

จุฬาลงกรณ์มหาวิทยาลัย
CHULALONGKORN UNIVERSITY